Available online at www.sciencedirect.com
SCIENCE DIRECT
Tetrahedron
ELSEVIER
Tetrahedron 62 (2006) 6471–6489

Intramolecular nucleophilic capture of radical cations by tethered hydroxy functions

Heinz D. Roth,* Torsten Herbertz, Ronald R. Sauers* and Hengxin Weng

Department of Chemistry and Chemical Biology, Rutgers University, Wright-Rieman Laboratories, New Brunswick, NJ 08854-8087, USA

Received 28 September 2005; accepted 6 December 2005
Available online 24 April 2006

Abstract—A range of systems bearing hydroxy functions tethered to the molecular framework gives rise to a family of interesting radical cations, **5**$^{\bullet+}$–**11**$^{\bullet+}$, upon electron transfer to photo-excited cyanoaromatics. Geraniol (**5**), nerol (**6**), citronellol (**7**), chrysanthemol (**8**), homochrysanthemol (**9**), *trans*-1-*o*-hydroxyphenyl-2-phenylcyclopropane (**10**), and *endo*-5-hydroxymethylnorbornene (**11**), generate a series of mono-, bi-, or tricyclic ethers via a series of four- to seven-membered transition states. Two of the radical cations, **5**$^{\bullet+}$ and **6**$^{\bullet+}$, undergo tandem cyclizations where 1,5- and/or 1,6-C–C cyclizations precede nucleophilic capture.

1. Introduction

The structures of organic radical cations and their reactions have attracted much attention during recent decades and continue to be the focus of intense interest.[1–13] Because of their dual nature, radical cations contain an unpaired spin and a positive charge, they may undergo a wide range of diverse reactions, including rearrangements[3–6] and sigmatropic shifts,[7] nucleophilic substitution or 'capture',[8,9] cycloadditions,[2d,10] as well as fragmentations[11] and cycloreversions.[12] Compared to the analogous reactions of the parent molecules, many radical cation reactions show a dramatic decrease in activation barriers,[11,13] one of the most striking aspects of radical cation chemistry.[3] Among the plethora of reactions the capture by nucleophiles has been investigated in detail.

As a result of their electron deficient nature radical cations are strong acids and are excellent targets for nucleophilic substitution or capture. A wide range of strained ring radical cations undergo nucleophilic substitution, i.e., backside attack with inversion of configuration.[8,9] The stereochemical requirements for this reaction are considered rigorous; molecular orbital calculations indicate that a trajectory close to 180° is critical.[14] Many of these substitutions occur at sterically encumbered carbons;[7,13] apparently, relief of ring strain significantly increases the driving force; this increase more than compensates for the steric hindrance.

The various factors governing regio- and stereochemistry of nucleophilic substitution on radical cations have been evaluated in a series of substrates that offer regiochemical competition within the target molecule. Not surprisingly, molecular orbital (MO) factors, particularly the nature of the singly occupied molecular orbital (SOMO) and the lowest unoccupied molecular orbital (LUMO), are of major importance. If MO factors allow more than one reaction, the thermodynamic stability of the resulting free radicals determines the outcome.[7b,c,15] Steric factors typically do not play a major role; in fact, several radical cations are captured by attack on highly congested centers.[7,13] However, at least one radical cation is captured selectively at the less encumbered site.[15] We illustrate the major factors in the following examples, which were chosen to differentiate unambiguously between potentially governing factors.

A simple system illustrating the role of molecular orbital effects is the radical cation of *trans*-1,2-dimethylcyclopropane. The unpaired spin density, SOMO and LUMO of this species are shown in Figure 1; both HOMO and LUMO have a node at C-3. Accordingly, this radical cation and likewise other 1,2-disubstituted cyclopropane radical cations are unreactive at C-3.[3b,16]

The radical cation of sabinene, **1**$^{\bullet+}$, contains a rigidly arranged vinylcyclopropane system; unpaired electron spin and charge are delocalized over four atoms, C-5, C-1, C-4, and C-4′; however, only two centers, C-1 and C-4′ have significant orbital coefficients in both HOMO and LUMO. Thus, nucleophiles should be able to attack **1**$^{\bullet+}$ either at the exocyclic alkene position or at the cyclopropane ring. In fact, nucleophilic attack occurs exclusively at the highly congested

Keywords: Electron transfer; Radical cation; Photochemistry; Intramolecular nucleophilic substitution; Tandem cyclization.
* Corresponding authors. Tel.: +1 732 445 5664; fax: +1 732 445 5312 (H.D.R.); tel.: +1 732 445 2626 (R.R.S.); e-mail addresses: roth@rutchem.rutgers.edu; sauers@rutchem.rutgers.edu

0040–4020/$ - see front matter © 2006 Elsevier Ltd. All rights reserved.
doi:10.1016/j.tet.2006.03.064

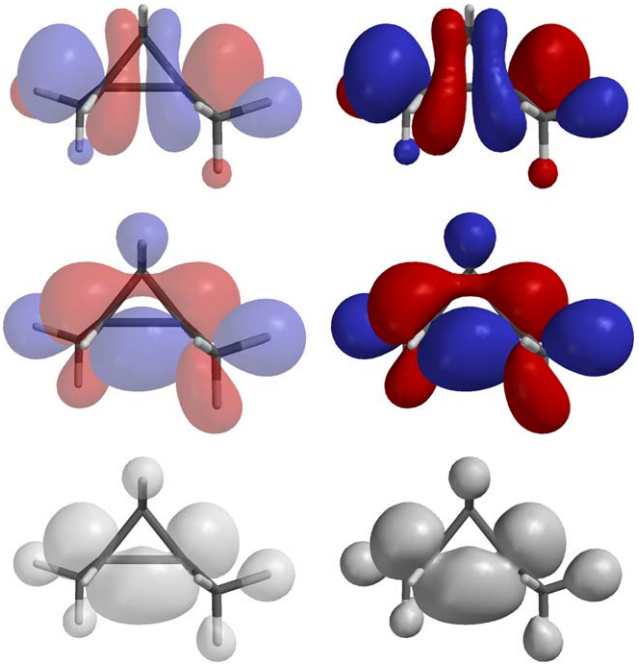

Figure 1. Stereoview of unpaired spin density (bottom), singly occupied molecular orbital (SOMO, center), and lowest unoccupied molecular orbital (LUMO, top) for the radical cation of *trans*-1,2-dimethylcyclopropane.[16]

quaternary cyclopropane carbon; this reaction is favored because (1) it gives rise to a more stable allylic free radical (→ **•1-A**-OCH_3) and (2) it occurs with complete release of ring strain.[7b]

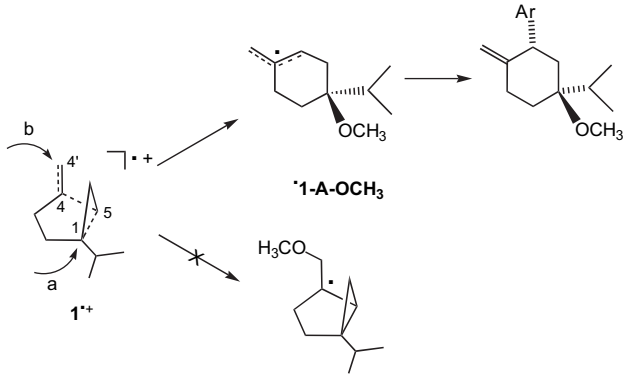

In contrast, tricyclo[4.3.1.$0^{1,6}$]deca-2,4-triene radical cation, **2**$^{•+}$, which formally has two pathways of nucleophilic substitution with relief of ring strain (a,b), fails to utilize either. The species has spin and charge density at C-2, C-5, and C-10 but is attacked exclusively at C-2/C-5 (c,d), retaining the significant ring strain in the products. The course of this substitution is determined by the large LUMO coefficients at C-2, C-5 in contrast to the absence of major LUMO coefficients at C-10 or at the bridgehead carbons, C-1 and C-6 (Scheme 1; Fig. 2).[17]

The role of steric factors is illustrated unambiguously by comparison of two tricyclane isomers, 2,3,3-trimethyltricyclo[2.2.1.$0^{2,6}$]heptane,[18] **3**, and 1,3,3-trimethyltricyclo[2.2.1.$0^{2,6}$]heptane,[15] **4**. Nucleophiles attack **3**$^{•+}$ and **4**$^{•+}$ exclusively at tertiary carbons, not the quaternary ones; this finding is ascribed to the formation of the more stable

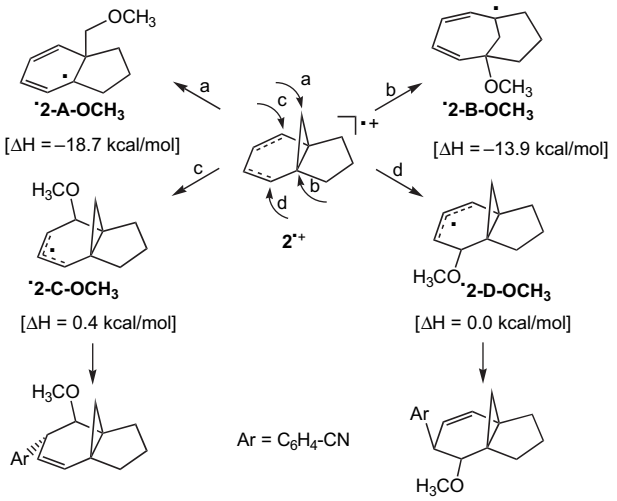

Scheme 1. Potential regioisomeric free radicals generated by nucleophilic addition/capture of tricyclo[4.3.1.$0^{1,6}$]deca-2,4-triene radical cation, **2**$^{•+}$, by methanol. The enthalpies of the corresponding truncated norcaradiene system are given in brackets.

tertiary radicals, **•3-A**-OCH_3 and **•4-A**-OCH_3. The symmetrical tricyclane, **3**, does not offer an unambiguous conclusion: attack at C-1/C-6 is unencumbered form either face. On the other hand, the chiral isomer, **4**, clearly illustrates the role of steric hindrance. One of the tertiary cyclopropane centers

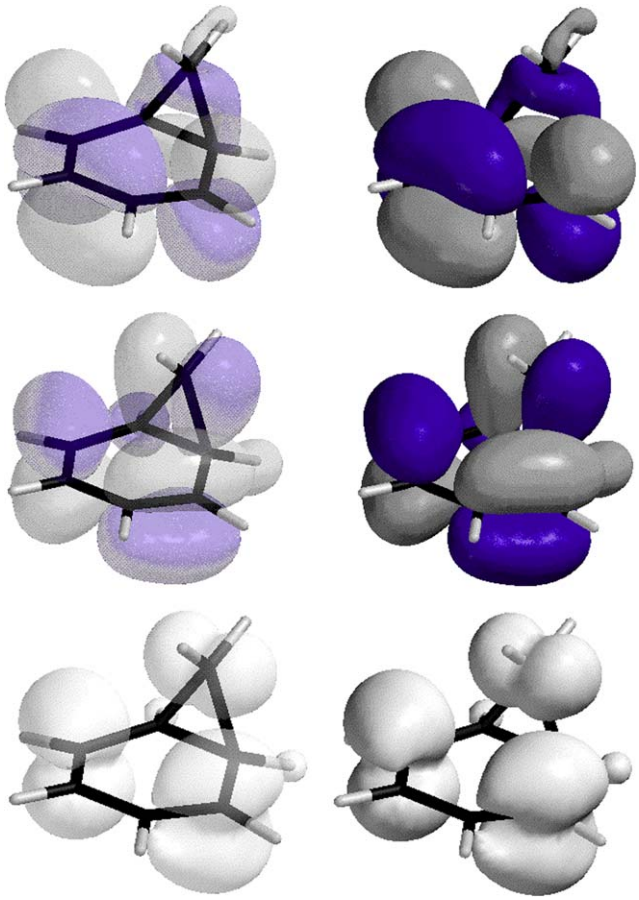

Figure 2. Stereoview of unpaired spin density (bottom), SOMO (center) and LUMO (top) for the radical cation of norcaradiene.[17]

of **4**, C-2, is a neopentyl type carbon whereas C-6 is sterically unencumbered. The result, exclusive attack at C-6, clearly establishes a significant role of steric hindrance in this system.[15] The intermediates of both reactions, **•3-A**-OCH_3 and **•3-A**-OCH_3respectively, form the final product by hydrogen, respectively, form the final product by hydrogen atom transfer to an adventitious acceptor.

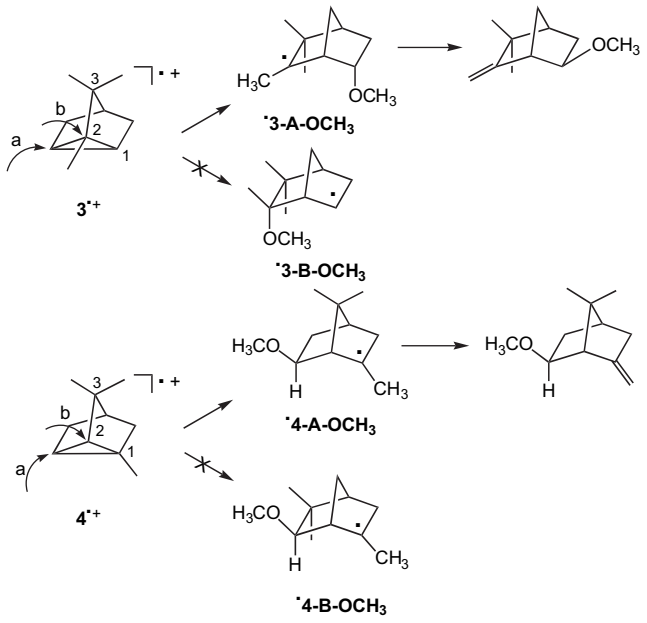

Three of the reactions discussed above, those of $\mathbf{1}^{\bullet+}$, $\mathbf{3}^{\bullet+}$, and $\mathbf{4}^{\bullet+}$, are 'genuine' substitution reactions, akin to an S_N2 reaction, albeit on substrates that are one electron shy of the diamagnetic prototype. These reactions involve backside attack with release of a leaving group, in each case a free radical that remains attached to the molecule. For these reactions, the trajectory of approach may be important.[14] The reaction of $\mathbf{2}^{\bullet+}$ is different as the nucleophile adds to, or is 'captured' by an 'empty p-orbital' or an electron deficient π-system. This reaction is akin to the second, product-forming step of an S_N1 reaction. The stereochemical requirements for this type of reaction may be less demanding.

We have an interest in the intramolecular variant of these reactions, i.e., nucleophilic substitution or capture of radical cations by hydroxy groups tethered to the centers bearing spin and charge. Compared to the more general case of capture by an external nucleophile the intramolecular case offers some intriguing features. Steric features, including conformational preferences, may play a significant role in the substitution by or capture of an intramolecular nucleophile. Particularly, introduction of ring strain is seen as a major potential impediment for the cyclization of such systems. In general, the factors may be similar to those governing other ring-forming reactions such as the Dieckman condensation[19] or intramolecular nucleophilic substitution of bifunctional compounds.[20] For example, the Dieckman condensation works well for five-, six-, and seven-membered rings, whereas larger rings require high-dilution techniques, a direct reflection of the conformationally encumbered transition states of such ring systems. Similarly, intramolecular S_N2 reactions proceed optimally via five- and six-membered transition states.

In order to probe various features of intramolecular reactions of radical cations with nucleophiles, we selected a series of substrates designed to cover a range of cases that would allow us to elucidate the principles governing this reaction type. For several of these species the tethered nucleophile has only a single possibility to react whereas in others it has the 'option' of attacking two or three different centers via different transition states with different driving forces and different barriers.

The systems chosen provide the opportunity to evaluate reactions proceeding via four- to eight-membered transition states, in several cases with intra-species competition. A four-membered transition state is actually realized in one system. Not surprisingly, several substrates utilize five- and six-membered transition states; both substitution and capture readily proceed via these common transition states. Three of our systems have the potential of reacting via seven-membered transition states; two radical cations react in this fashion, one actually in competition with other cyclizations. Finally, two radical cations offer the possibility of reaction via an eight-membered transition state without, however, using this pathway. Three of the systems studied contain three-membered rings; they were chosen for the additional driving force which relief of ring strain might provide.

The seven target molecules chosen for our investigation are listed in Chart 1; geraniol (**5**), nerol (**6**), citronellol (**7**), chrysanthemol (**8**), homochrysanthemol (**9**), *trans*-1-*o*-hydroxyphenyl-2-phenylcyclopropane (**10**), and *endo*-5-hydroxymethylnorbornene (**11**), generate a family of mono-, bi-, or tricyclic ethers via a series of four- to seven-membered transition states.

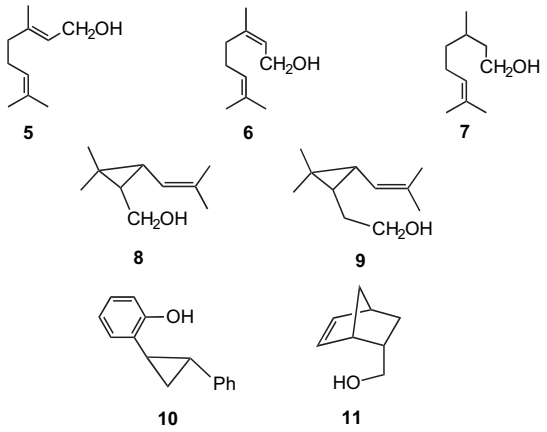

Chart 1. Target systems chosen for this study.

In all these systems the hydroxyl function serves as the nucleophile. This moiety is not a potent nucleophile in S_N2 reactions; for example, OH or COOH functions only undergo intramolecular substitution after being deprotonated. However, in reactions with radical cations, as well as carbocations, which are superacids as well as 'super electrophiles', the OH function is an efficient nucleophile. This is borne out by rates of nucleophilic capture, e.g., $k \sim 10^8\ l\ mol^{-1}\ s^{-1}$, for the capture of phenylcyclopropane radical cation by methanol.[13d]

In selected cases, these experimental findings are viewed in the light of molecular orbital calculations with ab initio or density functional theory (DFT) methods (vide infra). In addition to the geometries of selected intermediates, especially key bond lengths, we have generated pictorial representations of unpaired spin densities (ρ), the singly occupied molecular orbitals (SOMOs), and the lowest unoccupied (LU) MOs. The unpaired spin densities on carbon determine the hyperfine coupling constants (hfcc) of free radicals and radical ions; in most cases the signs and magnitudes of hfccs provide the only available *experimental* evidence for the structures of these intermediates.

2. Method of generation

The radical cations of the target molecules, **5**–**11**, were generated by electron transfer to a photo-excited sensitizer or a sensitizer/co-sensitizer system (e.g., Scheme 2, Eq. 1–3). The intramolecular nucleophilic substitution or capture of radical cations, $\mathbf{5}^{\bullet+}$–$\mathbf{11}^{\bullet+}$, give rise initially to bifunctional radical cations containing an oxonium ion and a localized or delocalized free radical. Rapid deprotonation of the oxonium ions leaves free radicals (Eq. 4), which have several potential reactions available, including aromatic substitution on the sensitizer radical anion (Eq. 6); reduction by return electron transfer (RET) from the sensitizer radical anion, followed by protonation (Eq. 5); or hydrogen abstraction from an adventitious hydrogen atom donor (Eq. 7). In some cases, the neutral radicals may form alkenes by hydrogen transfer to a suitable hydrogen atom acceptor (Eq. 8).

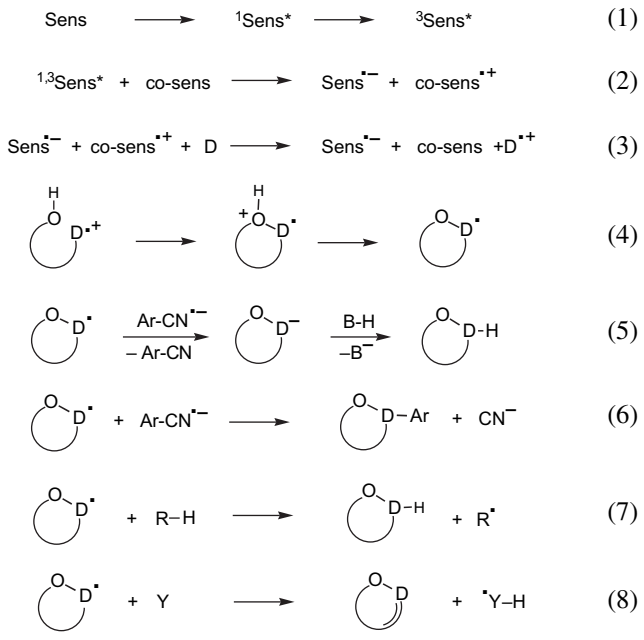

Scheme 2. Photo-induced electron transfer reactions of donor molecules bearing a tethered hydroxyl function.

The free energy of formation of radical ion pairs generated by electron transfer between a donor and an acceptor (Scheme 2; Eq. 3) is determined by the excited state energy, ($E_{0,0}$), the reduction potential of the acceptor, $E^0_{(A^-/A)}$, the oxidation potential of the donor, $E^0_{(D/D^+)}$, and a term accounting for ion pairing (Eqs. 9 and 10).[21] In a modified formulation of the Rehm–Weller equation (Eq. 10), [2.6 eV/ε−0.13 eV] is an empirical term accounting for solvents of different polarity,[21a] when the excitation energy and redox potentials are measured in acetonitrile; in polar solvents, $e^2/\varepsilon a$ has a value of ~0.06 eV. Typically, a driving force, $-\Delta G_{ET} \geq 0.5$ eV, is sufficient to generate solvent separated radical ion pairs (SSRIP).

$$-\Delta G^0 = E_{(0,0)} - E^0_{(D/D^+)} + E^0_{(A^-/A)} - e^2/\varepsilon a; \quad (9)$$

$$-\Delta G^0_{SSRIP} = E_{(0,0)} - E^0_{(D/D^+)} + E^0_{(A^-/A)} - [2.6\,\text{eV}/\varepsilon - 0.13\,\text{eV}] \quad (10)$$

The oxidative power of an acceptor/sensitizer can be gauged by its excited state reduction potential,

$$^*E^0_{(A^-/A)} = E^0_{(0,0)} + E^0_{(A^-/A)} \quad (11)$$

Photosensitizers used in this study include 1,4-dicyanobenzene (**DCB**; $E^0_{(0,0)}$=4.29 eV, $E^0_{(A^-/A)}$=−1.6 V; $^*E^0_{(A^-/A)}$=2.7 V), 9,10-dicyanoanthrazene (**DCA**; $E^0_{(0,0)}$=2.88 eV, $E^0_{(A^-/A)}$=−0.9 V; $^*E^0_{(A^-/A)}$=2.0 V), and triphenylpyrylium tetrafluoroborate (**TPP**; $^1E^0_{(0,0)}$=2.8 eV, $E^0_{(A^-/A)}$=−0.29 V; $^1E^0_{(A^-/A)}$=2.5 V; $^3E^0_{(A^-/A)}$=2.0 V). Their oxidative strength should be sufficient to oxidize all electron donors studied. Accordingly, all photoreactions discussed here can be viewed as radical cation reactions. Details will be given as appropriate.

3. Results

Photo-induced one-electron transfer causes the terpene geraniol, **5**, to undergo an interesting five-center C–C cyclization. With 1,4-dicyanoanthracene/biphenyl (**DCA/BP**) as sensitizer/co-sensitizer, a primary stereoselective C–C cyclization is followed by intramolecular hydrogen transfer yielding **12**. With 9,10-dicyanobenzene/phenanthrene (**DCB/Ph**) the C–C cyclization is less selective and is followed by a second five-center cyclization, capture of C_7 by the alcohol function. Overall, this reaction generates a series of cis- and trans-fused 3-oxabicyclo[3.3.0]octanes, **13**.[22a]

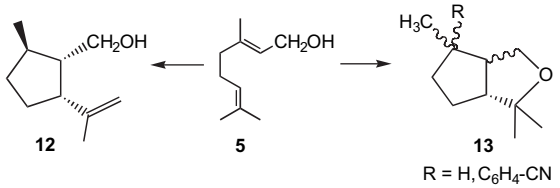

The *Z*-isomer of **5**, nerol, **6**, undergoes a range of significantly different reactions. Irradiation of **DCA/BP** in the presence of **6** gives rise to two monocyclic and two bicyclic ring systems, **14**–**17**. The formation of two products, 1,2,2-cyclopentylacetaldehyde, **14**, and 4-cyanophenyl-5,7,7-trimethyl-2-oxabicyclo[3.2.1]octane, **15**, appears compatible with a five-center C–C cyclization; one product, 2,2,6-trimethyl-7-oxabicyclo[4.2.0]octane, **16**, arises by a 'tandem'

cyclization, initiated by a six-center C–C ring closure, which is followed by a four-center nucleophilic capture. Finally, the oxepene, 4-methyl-7-isopropyl-3-oxepene, **17**, requires a seven-center intramolecular nucleophilic capture. With the **DCB/Ph** pair, **6** undergoes *Z*-to-*E* isomerization, and forms aldehyde, **14**, in addition to traces of **17** and tandem cyclization product, **15**.[22b]

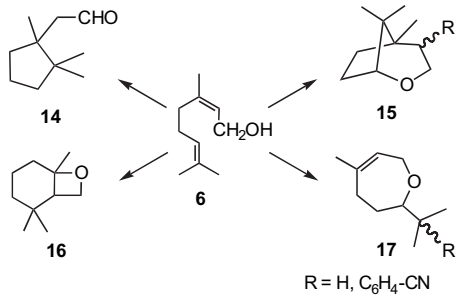

Irradiation of **DCA/BP** as sensitizer/co-sensitizer in acetonitrile in the presence of citronellol, **7**, which has only one olefinic function (i.e., dihydro-**6**), gives rise to the oxepane derivative **18** (i.e., dihydro-**17**) in good yield, confirming the dimethylethene function as a suitable electron donor under these conditions. This reaction requires a seven-center intramolecular nucleophilic capture.[22b]

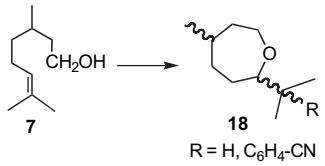

The OH function of chrysanthemol [1-(2-hydroxy-ethyl)-2,2-dimethyl-3-(2-methyl-1-propenyl)-cyclopropane] radical cation, $\mathbf{8}^{\bullet+}$, could attack the three-membered ring by nucleophilic substitution or the olefinic side chain by nucleophilic capture. Only the capture reaction is observed forming ring-expanded aryl-substituted products of type **19**.[23]

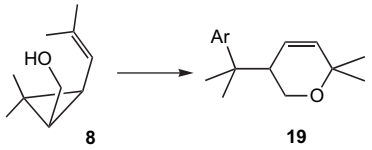

Homochrysanthemol [1-(3-hydroxy-propyl)-2,2-dimethyl-3-(2-methyl-1-propenyl)-cyclopropane] radical cation, $\mathbf{9}^{\bullet+}$, like the lower homolog $\mathbf{8}^{\bullet+}$, has two possible pathways for the OH function to react with the electron deficient moiety. The extended tether diverts the point of attack completely to the three-membered ring, giving rise to aryl-substituted products of type **20**, as well as a free radical dimer.[24]

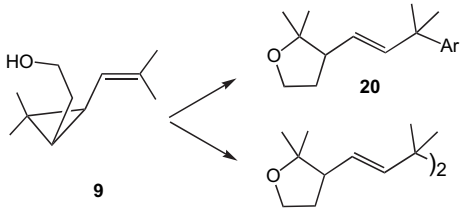

The electron transfer photochemistry of *trans*-**10** was carried out with triphenylpyrylium tetrafluoroborate (**TPT**). Sensitized irradiation of *trans*-**1** through Pyrex in methylene chloride under argon gave rise to 2-phenyl-2*H*-benzopyran, **21**, as the sole product (15% conversion after 5 h, 97% material balance).[25]

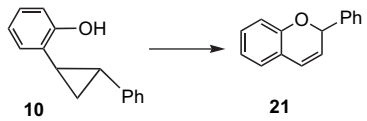

Finally, irradiation of **DCA/BP** as sensitizer/co-sensitizer in acetonitrile in the presence of *endo*-5-hydroxymethylnorbornene, **11**, generated the tricyclic ether, 4-oxatricyclo-[4.2.1.03,7]nonane, **22**, in moderate yield.[22]

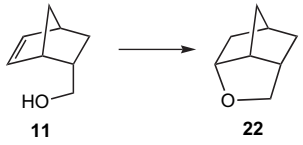

4. Discussion

We will discuss the radical cations whose reactions are being treated here in three groups. First we consider the terpene radical cations, $\mathbf{5}^{\bullet+}$, $\mathbf{6}^{\bullet+}$, and $\mathbf{7}^{\bullet+}$; they are of particular interest because $\mathbf{5}^{\bullet+}$ and $\mathbf{6}^{\bullet+}$ provide a competition between C–C and C–O bond formations. The second group, comprised of chrysanthemol and homochrysanthemol radical cations, $\mathbf{8}^{\bullet+}$ and $\mathbf{9}^{\bullet+}$, offers two different competing pathways involving nucleophilic substitution and capture. Finally, we discuss two radical cations that undergo 1,5-cyclizations, at least formally. The diarylcyclopropane radical cation, $\mathbf{10}^{\bullet+}$, poses an intriguing structure/reactivity problem whereas $\mathbf{11}^{\bullet+}$ probes the interesting aspect of *endo* attack on a norbornene radical cation.

4.1. Geraniol and nerol radical cations—competing C–C and C–O cyclizations

The radical ions of geraniol and nerol undergo both C–C and C–O cyclizations. Both processes generate bifunctional radical cations. The difference lies in the fact that the C–O closures generate a 'product' containing an oxonium ion, which is readily deprotonated, and is not suitable for further cyclization. In contrast, the species resulting from C–C closure contain a carbocationic site; intermediates of this type are less easily deprotonated and are still suitable/susceptible for nucleophilic capture. These species have the potential for tandem cyclization: both $\mathbf{5}^{\bullet+}$ and $\mathbf{6}^{\bullet+}$ undergo 1,5- and/or 1,6-C–C cyclizations, which are followed by nucleophilic capture.

Because of the *E*-geometry of geraniol the nucleophilic center of its radical cation, $\mathbf{5}^{\bullet+}$, can only serve in this capacity after having been 'released' or 'unlocked', for example, by an addition at C-2. Accordingly, it was not surprising that $\mathbf{5}^{\bullet+}$ reacted by bond formation between C-2 and C-6, i.e., via a five-membered transition state; the resulting

bifunctional radical cation, *cis*-5-C–Ccy-**5**$^{\bullet+}$, is a ditertiary species and should be relatively stable. Indeed, with **DCA/BP** as sensitizer/co-sensitizer, the reaction was arrested at the stage of the monocyclic intermediate. The high stereospecificity observed with **DCA/BP** was unexpected: only the cis-fused ring was formed and only one stereoisomer of **12** was generated.[22a]

In order to explain the (unexpected) stereospecificity of ring closure, we note the limited driving force for electron transfer. The reduction potential of **DCA** ($E_{(A^-/A)}$=−0.9 V), and its low excited state energy ($E_{0,0}$=2.88 eV) render the oxidation of **5** by ^{1}**DCB*** mildly exergonic ($\Delta G_{ET}\sim$−0.1 eV) in CH_3CN and slightly endergonic ($\Delta G_{ET}\sim$+0.2 eV) in CH_2Cl_2. Accordingly, the radical ions **DCA**$^{\bullet-}$ and **5**$^{\bullet+}$ can be generated only as tight ('sandwich') ion pairs, causing the substituents at the developing bonds to move 'outward', away from the counter ion, resulting in the observed cis-stereochemistry. The orientation of the methyl group trans to the isopropenyl function was explained via triplet return electron transfer, generating a biradical, *cis*-5-C–Ccy-**5**$^{\bullet\bullet}$; a 1,5-intramolecular (suprafacial) hydrogen shift readily accounts for the trans-stereochemistry.[22a]

Return electron transfer in triplet radical ion pairs has been of great interest for several decades.[26] Of special interest are systems that undergo rearrangement during the consecutive lifetimes of radical ions and triplet states or biradicals.[27] Geraniol belongs to a group of systems where the radical cation undergoes a major structure change, **5**$^{\bullet+}$ to *cis*-5-C–Ccy-**5**$^{\bullet+}$, a species corresponding to a non-Kekule structure in the ground state.[27] The reorganized structure is retained upon electron return (*cis*-5-C–Ccy-**5**$^{\bullet+}$ to *cis*-5-C–C-cy-**5**$^{\bullet\bullet}$), then reverts to a Kekule structure with a minor change in structure, a 1,5-H shift forming *cis*,*trans*-**12**.[27] Details of this interesting topic go beyond the scope of this article.

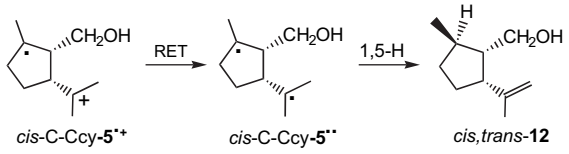

For the reaction of **5** with the **DCB/Ph** pair, electron transfer from the donor substrates to ^{1}**DCB*** dicyanobenzene ($E^0_{(0,0)}$=4.29 eV, $E^0_{(A^-/A)}$=−1.6 V; *$E^0_{(A^-/A)}$=2.7 V) should be efficient, regardless of the solvent. Under these conditions the reaction takes a different course in two respects: (a) the C–C ring closure is much less stereospecific and (b) the reaction proceeds past the stage of 5-C–Ccy-**5**$^{\bullet+}$, as the partial positive charge at C-7 is captured by the hydroxy function, completing a tandem cyclization.

Because the electron transfer reaction is comfortably exergonic (−$\Delta G_{ET}\sim$0.8 eV), the ion pair, **DCA**$^{\bullet-}$–**5**$^{\bullet+}$, is generated as a solvent separated radical ion pair without intra-pair interactions that would affect the stereochemistry of C–C closure. The resulting bicyclic free radicals, *Z*- or *E*-**5**$^{\bullet}$, react by aromatic substitution[28] (Scheme 2, Eq. 6) as well as by hydrogen abstraction (Scheme 2, Eq. 7)—neither reaction has any pronounced stereochemical preference. The lack of specificity in this reaction turned product separation into a challenge and has precluded synthetic utility, at least to date.[22a]

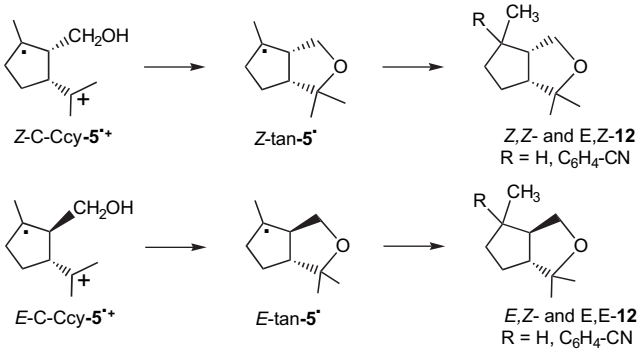

The structural features of the three key radical cations, **5**$^{\bullet+}$, *cis*-5-C–Ccy-**5**$^{\bullet+}$, and 5,5-tan-**5**$^{\bullet+}$, were calculated using density functional theory (DFT) methods (Fig. 3); in order to allow a comparison of their calculated enthalpies the proton on the oxonium ion, 5,5-tan-**5**$^{\bullet+}$ was not allowed to dissociate. The first (C–C) cyclization is endergonic by 2.5 kcal mol^{-1}, whereas the second (O–C) cyclization is exergonic by 4.3 kcal mol^{-1}. The deprotonation of the oxonium function lowers the enthalpy further, rendering the tandem cyclization irreversible.

A comparison of the spin and charge density distributions in the three species is illuminating. The parent radical cation, **5**$^{\bullet+}$, has unpaired spin density in both alkene groups; the dimethylethylene carbons bear similar spin densities (ρ_6=0.212, ρ_7=0.213), whereas the hydroxyl group apparently polarizes the partial double bond between C-2 and C-3 (ρ_2=0.272, ρ_3=0.096). In the first cyclization product, *cis*-5-C–Ccy-**5**$^{\bullet+}$, the spin is distributed between C-3 (ρ=0.461) and C-7 (ρ=0.542). Upon closing the second ring, forming 5,5-tan-**5**$^{\bullet+}$, the unpaired spin becomes localized on C-7 (ρ=0.958) whereas the charge is placed on the oxygen, polarizing the bonds to the adjacent atoms (C_1=0.339, C_7=0.265, O–H=0.474).

Interestingly, under different reaction conditions, using 1,4-**DCB/Ph** in anionic micellar solution, the acetate of **5** (**23**) as well as the sesquiterpene and diterpene acetates, farnesyl (**24**) and geranylgeraniol acetate (**25**), undergo 1,6-cyclizations, generating six-membered mono-, bi-, and tricyclic

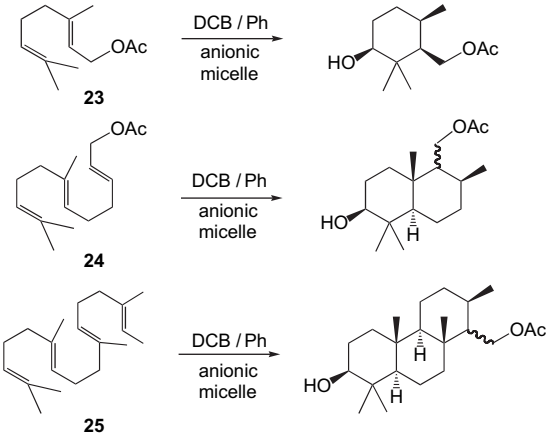

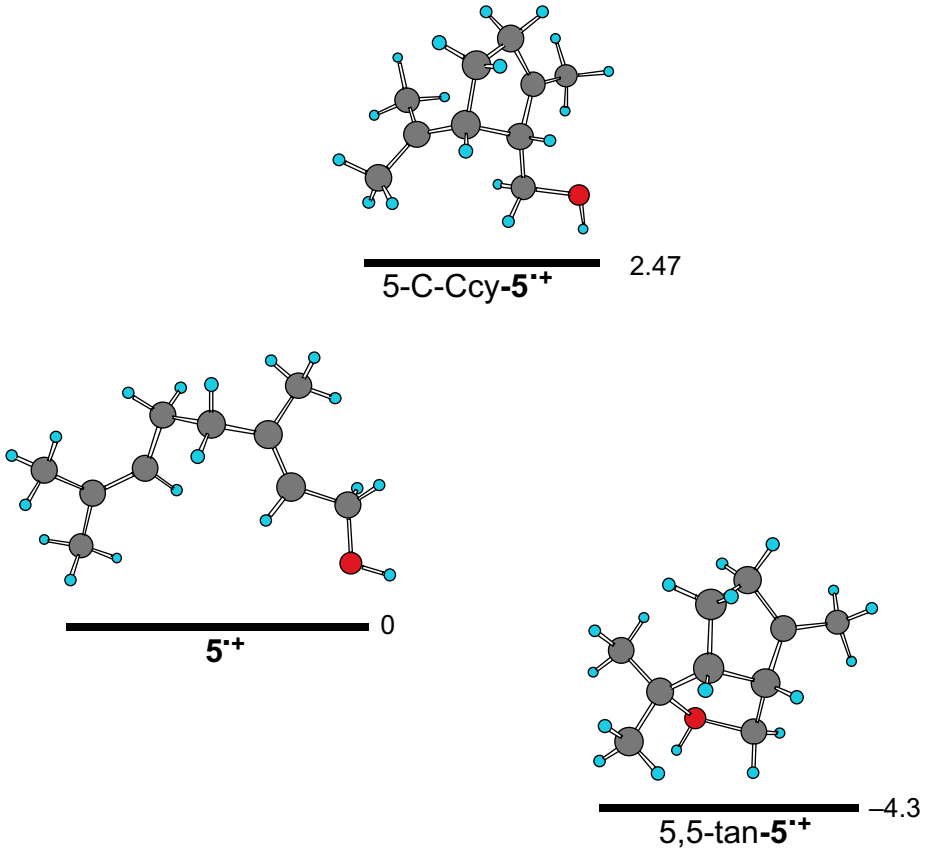

Figure 3. Chem-3D models of geraniol radical cation, $\mathbf{5}^{\bullet+}$, and two isomers generated by C–C cyclization, *cis*-5-C–Ccy-$\mathbf{5}^{\bullet+}$, and tandem cyclization, 5,5-tan-$\mathbf{5}^{\bullet+}$, respectively. The geometries were calculated by DFT methods using the 6-31G* basis set; relative enthalpies (kcal mol^{-1}) are indicated.

products, respectively.[29] The bi- and tricyclic products are trans-fused and all are hydroxylated in anti-Markovnikov fashion; apparently the radical ions are terminated by water. These reactions are the first examples of photochemically initiated biomimetic terpenoid cyclizations.

The *Z*-isomer of $\mathbf{5}^{\bullet+}$, nerol radical cation, $\mathbf{6}^{\bullet+}$, cannot be expected to undergo cyclization between C-2 and C-6 because the conformer required for this conversion appears to be seriously hindered by the steric repulsion between the hydroxymethyl group and the terminal dimethylethylene moiety. For $\mathbf{5}^{\bullet+}$, a helical arrangement can relieve the less severe steric repulsion between the hydrogens at C_2 and C_6 without compromising their required proximity. However, the helical conformer of $\mathbf{6}^{\bullet+}$ is still severely hindered, so that alternative reactions must be expected. Indeed, **6** does not generate any product derived by bond formation between C-2 and C-6.[22b]

However, other cyclizations also have steric challenges. For example, products **14** and **15** result from five-carbon C–C cyclization between C-3 and C-7, yielding 5-C–Ccy-$\mathbf{6}^{\bullet+}$. Although this approach avoids the C-2–C-6 crowding, the C-3 onto C-7 approach does not appear significantly less crowded. Perhaps as a result of this steric impediment $\mathbf{6}^{\bullet+}$ undergoes the most varied ring formations of any system discussed here. The various reactions of $\mathbf{6}^{\bullet+}$ result in the formation of five-, six-, and seven-membered rings and support nucleophilic capture via four-, six-, and seven-membered transition states. These products are compatible with primary cyclizations yielding 5-C–Ccy-$\mathbf{6}^{\bullet+}$, 6-C–Ccy-$\mathbf{6}^{\bullet+}$, and 7-O–Ccy-$\mathbf{6}^{\bullet+}$, respectively; the latter would be deprotonated readily to 7-O–Ccy-$\mathbf{6}^{\bullet}$.[22b]

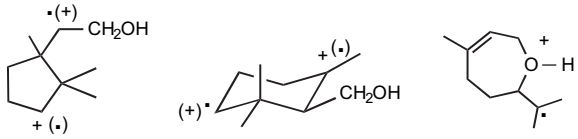

With **DCB/Ph** as sensitizer/co-sensitizer, **6** forms aldehyde **14** as the major product and undergoes *Z*-to-*E* isomerization. This cyclization is not only sterically disadvantaged, but it places spin and charge on two secondary carbons in the putative intermediate. For the conversion of 5-C–C-cy-$\mathbf{6}^{\bullet+}$ to **14** we consider triplet electron return and an intramolecular (suprafacial) 1,5-hydrogen shift from the β-carbon of the side chain (C_2) to the cyclopentyl ring (C_6) in the resulting biradical, 5-C–Ccy-$\mathbf{6}^{\bullet\bullet}$; this species also explains the observed *Z*-to-*E* isomerization.[26,27] The bicyclic ether, **15**, suggests that 5-C–Ccy-$\mathbf{6}^{\bullet+}$, in analogy to 5-C–Ccy-$\mathbf{5}^{\bullet+}$, undergoes intramolecular nucleophilic capture completing a tandem cyclization. The resulting 5,6-tan-$\mathbf{6}^{\bullet}$ generates **15** by hydrogen abstraction (cf., Scheme 2, Eq. 7).[22b]

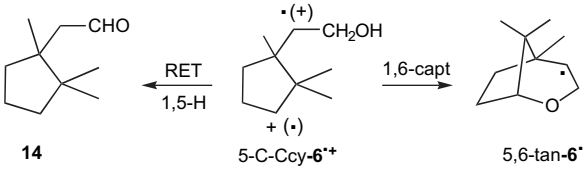

With the **DCA/BP** as sensitizer/co-sensitizer, **6** is converted to **14**, **16**, and **17**. The intermediate leading to **16** is a cyclohexane-1,4-diyl system, 6-C–Ccy-**6**$^{\bullet+}$, formed by bond formation between C_2 and C_7; spin and charge are localized on a secondary and tertiary carbon, respectively. This type of system contains spin and charge in two parallel p-orbitals; this arrangement allows ready delocalization, thereby stabilizing the species.[30] Interestingly, 6-C–Ccy-**6**$^{\bullet+}$ undergoes nucleophilic capture of the tertiary carbon by the alcohol function via a four-membered transition state. The conversion of the 7-oxabicyclo[4.2.0]octan-4-yl radical, 6,4-tan-**6**$^{\bullet}$, to **16** by hydrogen abstraction (cf., Scheme 2, Eq. 7) is unexceptional. The formation of 6,4-tan-**6**$^{\bullet}$ from 6-C–Ccy-**6**$^{\bullet+}$ is significant as the only example of oxetane formation from a radical cation.[22] The reason for the general lack of specificity observed for **6**$^{\bullet+}$ may well lie in the sterically less demanding nature of nucleophilic capture and C–C bond formations between two trisubstituted, sp^2 hybridized carbons.[22b]

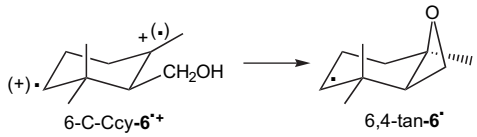

Finally, the hydroxymethyl group of **6**$^{\bullet+}$ interacts with the dimethylethylene function by forming the oxepene system, apparently by nucleophilic capture of C_6. The *Z*-arrangement of **6**$^{\bullet+}$ causes the hydroxy function to reside in the general vicinity of the molecule's 'tail end', allowing nucleophilic capture with formation of 7-O–Ccy-**6**$^{\bullet+}$. The transition state appears sterically congested, but it may be possible to arrange the seven centers C_6 through O in a quasi-boat that will reduce steric repulsion yet facilitate capture of C_6 by the OH function.[22] Formally, **6**$^{\bullet+}$ also has the potential to form an eight-membered ring system, but no product of this structure type was observed.[22b]

These results show that the potential hypersurface of nerol radical cation is significantly more complicated than that of **5**$^{\bullet+}$. The products suggest three primary cyclized species, 5-C–Ccy-**6**$^{\bullet+}$, 6-C–Ccy-**6**$^{\bullet+}$, and 7-O–Ccy-**6**$^{\bullet+}$, and two species resulting from tandem cyclization, 5,5-tan-**6**$^{\bullet+}$ and 6,4-tan-**6**$^{\bullet+}$, in addition to the parent radical cation, **6**$^{\bullet+}$. In order to gain additional insight into this potential surface, the key radical cations were probed using density functional theory (DFT) methods. As was the case for the intermediates derived from **5**, the oxonium protons were not 'allowed' to dissociate.

The calculations yielded five of the radical cations considered as likely intermediates. The cyclized species, 6-C–Ccy-**6**$^{\bullet+}$ and 7-O–Ccy-**6**$^{\bullet+}$, lie 9.96 kcal mol^{-1} and 8.85 kcal mol^{-1}, respectively, above **6**$^{\bullet+}$ (ΔH=0) and, thus, should be accessible during its lifetime. The products of tandem cyclization, 5,5-tan-**6**$^{\bullet+}$ (ΔH=7.97 kcal mol^{-1}) and 6,4-tan-**6**$^{\bullet+}$ (ΔH=11.70 kcal mol^{-1}), appear likewise accessible; deprotonation of the oxonium functions should lower the free enthalpies further, rendering the second cyclizations essentially irreversible. However, the calculations revealed one irreconcilable discrepancy with the simple mechanism considered: the putative precursor, 5-C–Ccy-**6**$^{\bullet+}$, for the major product (**14**) proved to be elusive. The approach of carbon atoms C-3 and C-7 is connected with a steep rise in energy due to the interference of the alkyl groups, rendering the formation of 5-C–Ccy-**6**$^{\bullet+}$ highly unfavorable. Accordingly, we searched for additional pathways leading from **6**$^{\bullet+}$ to **14**.

We noted that in the lowest energy conformer of **6**$^{\bullet+}$ one of the H atoms attached to C-1 is pointing inward, quasi poised for a hydride shift to C-6. This shift would lead to an intermediate, 6,1-H-**6**$^{\bullet+}$, containing an allylic free radical tethered to a tertiary carbocation. Rotational reorganization of the tether would allow cyclization between C-3 and C-7, yielding enol-**14**$^{\bullet+}$. Return electron transfer from the counter ion followed by tautomerization would complete a pathway to the major product, **14**, which potentially is lower in energy. In contrast to the conversion of **6**$^{\bullet+}$ to 5-C–Ccy-**6**$^{\bullet+}$, the hydride shift precedes the cyclization step in the newly considered pathway.

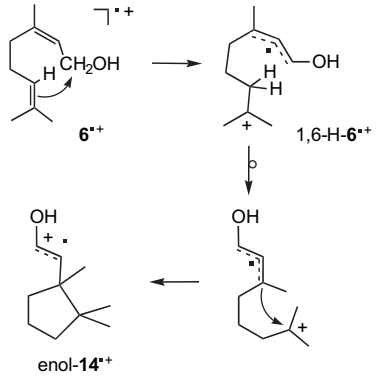

An examination of the proposed pathway by density functional calculations revealed the hydride shift to be exergonic; the corresponding transition state lies only 2.7 kcal mol^{-1} above **6**$^{\bullet+}$. Furthermore, the cyclization of 1,6-H-**6**$^{\bullet+}$ to enol-**14**$^{\bullet+}$ is endergonic by only 0.13 kcal mol^{-1}. These energetic features readily explain why **14** is obtained as the major product. The pertinent structures delineating the hydride shift are shown in Figure 4.

The hydride shift revealed by the calculations is interesting because it converts a bifunctional ('distonic') species in which spin and charge occupy separate regions of the molecular framework into a species in which spin and charge share the same pi system. In general, hydride shifts in radical cations are not without precedent; several rigid radical cations undergo stereospecific sigmatropic shifts. For example, the puckered ions, *anti*- and *syn*-5-methyl-**26**$^{\bullet+}$, undergo stereospecific hydride or methyl migration, respectively, forming 1-methylcyclopentene radical cation, **27**$^{\bullet+}$, as well as the 3-methyl isomer, **28**$^{\bullet+}$.[31]

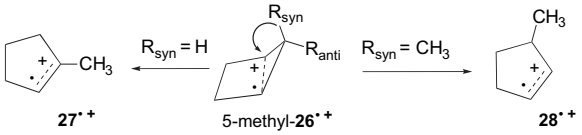

Similarly, sabinene radical cation, **1**$^{\bullet+}$, undergoes a stereospecific [1,3] shift to β-phellandrene radical cation, **29**$^{\bullet+}$, with high retention of optical purity whereas α-thujene

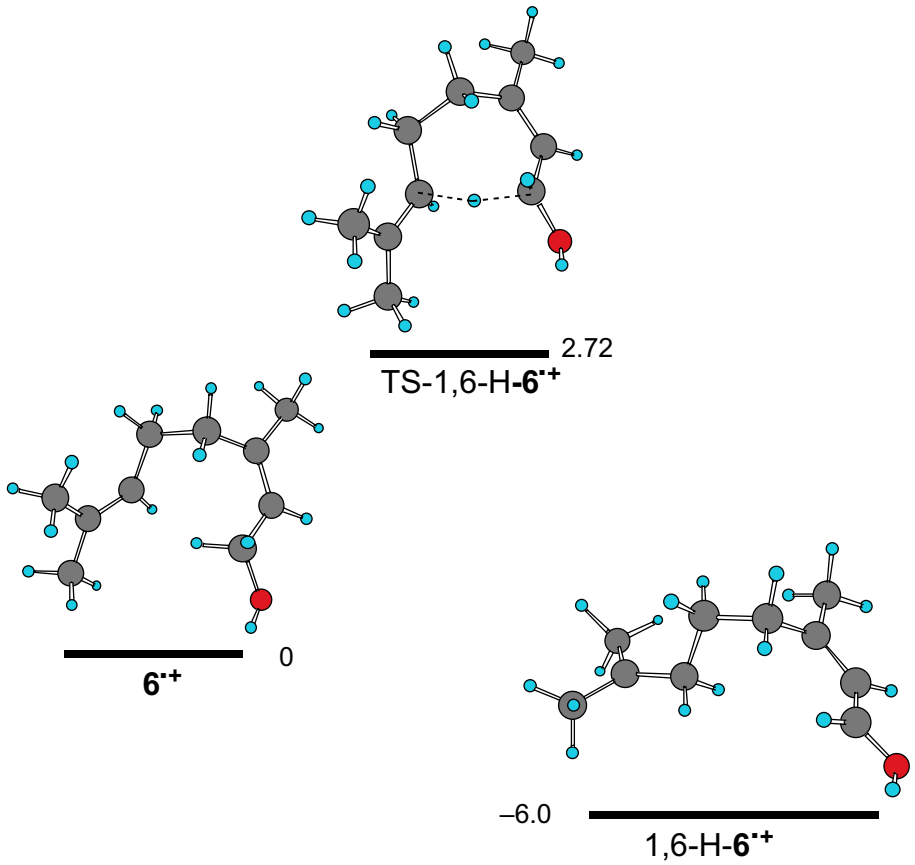

Figure 4. Chem-3D models of nerol radical cation, $\mathbf{6}^{\bullet+}$, an isomer generated by H-shift, 1,6-H-$\mathbf{6}^{\bullet+}$, and the transition state for the H-shift, TS-1,6-H-$\mathbf{6}^{\bullet+}$. The geometries were calculated by DFT methods (6-31G* basis set); relative enthalpies (kcal mol^{-1}) are indicated.

radical cation (not shown) undergoes competing [1,3] and home-[1,5] shifts to α-phellandrene radical cation.[7c] In these examples radical cations containing spin and charge in a lengthened cyclopropane 'sigma' bond are converted into species in which spin and charge share the same pi system.

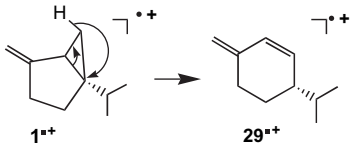

The high barrier connected with the putative ring closure of $\mathbf{6}^{\bullet+}$ to 5-C–Ccy-$\mathbf{6}^{\bullet+}$ affects the overall mechanism further as it eliminates the 'logical' precursor for the tandem cyclization product, 5,6-tan-$\mathbf{6}^{\bullet+}$. The newly uncovered species is not bifunctional and, therefore, cannot undergo a second ring closure. The possibility of yet another hydride shift, generating 5,6-tan-$\mathbf{6}^{\bullet+}$ from enol-$\mathbf{14}^{\bullet+}$, is remote because of the prohibitive enthalpy (ΔH=+13.84 kcal mol^{-1}) of this reaction.

A comparison of the spin and charge density distributions in $\mathbf{6}^{\bullet+}$ and the diverse radical cations derived from it provides additional insights. The parent radical cation, $\mathbf{6}^{\bullet+}$, has unpaired spin density in both the alkene groups; the spin densities of both the groups are slightly polarized (ρ_6=0.167, ρ_7=0.212; ρ_2=0.232, ρ_3=0.137); the hydroxyl group affects the spin density to a lesser degree than for $\mathbf{5}^{\bullet+}$. The product generated by hydride shift, 1,6-$\mathbf{H}$-$\mathbf{6}^{\bullet+}$, has an unusual distribution of spin and charge; the spin is located mainly on C-7 (ρ_7=0.632) and to a lesser extent on C-1 (ρ_1=0.214) and C-3 (ρ_3=0.210) whereas the charge is distributed between C-1 (0.156) and C-3 (0.205) and C-7 (0.211). Cyclization product 6-C–Ccy-$\mathbf{6}^{\bullet+}$ bears spin density mainly at C-6 (ρ_6=0.758) and C-3 (ρ_3=0.322) whereas the charge has its greatest density at C-3 (0.273), which interacts with the hydrogen atoms at C-2, C-4, and the adjacent methyl group; finally, 7-O–Ccy-$\mathbf{6}^{\bullet+}$ has the unpaired spin essentially localized at C-7 (ρ_7=0.667) and the charge is placed on the oxygen, polarizing the bonds to the adjacent atoms, C-6 (0.175), C-1 (0.266), C-3 (0.197), and O–H (0.447). Tandem cyclization product 5,6-tan-$\mathbf{6}^{\bullet+}$ has the unpaired spin localized on C-2 (ρ_2=0.944) whereas the charge on the oxygen atom polarizes the bonds to the adjacent atoms, C-1 (0.323), C-6 (0.265), and O–H (0.473). Finally, 6,4-tan-$\mathbf{6}^{\bullet+}$ has the unpaired spin localized on C-6 (ρ_6=1.019) whereas the charge on the oxygen atom polarizes the bonds to the adjacent atoms, C-1 (0.398), C-3 (0.277) and the adjacent methyl carbon (0.142), and O–H (0.471). The relative enthalpies of the key intermediates are summarized in Figure 5.

Our interest in citronellol, **7**, a terpene with only one double bond, not likely to be an excellent electron donor, arose from the unusual reaction of $\mathbf{6}^{\bullet+}$. This reaction might suggest that the terminal dimethylethylene group serves as the primary electron donor. This possibility can be probed by

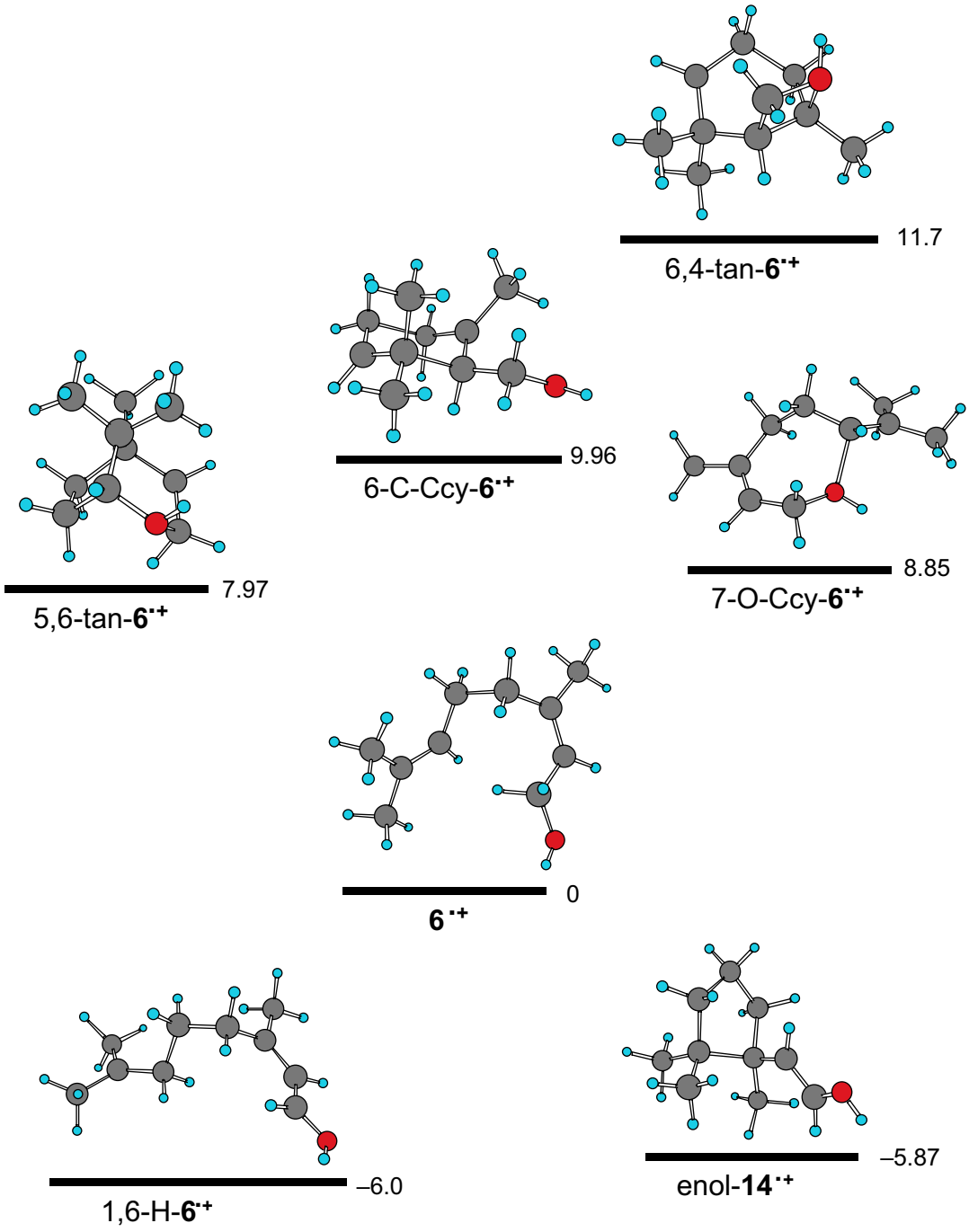

Figure 5. Chem-3D models of nerol radical cation, $\mathbf{6}^{\bullet+}$, and isomers: (i) generated by C–C or O–C cyclization, 6-C–Ccy-$\mathbf{6}^{\bullet+}$ and 7-C–Ocy-$\mathbf{6}^{\bullet+}$, (ii) resulting from tandem cyclization, 5,6-tan-$\mathbf{6}^{\bullet+}$ and 6,4-tan-$\mathbf{6}^{\bullet+}$, and (iii) formed by a H-shift, 1,6-H-$\mathbf{6}^{\bullet+}$, and subsequent cyclization, enol-$\mathbf{14}^{\bullet+}$, respectively. The geometries were calculated by DFT methods with the 6-31G* basis set; relative enthalpies (kcal mol^{-1}) are indicated.

investigating the electron transfer photochemistry of citronellol, **7**, in essence the dihydro-derivative of **6**. Irradiation of **DCA/BP** in the presence of **7** gives rise to oxepane **18** (i.e., dihydro-**17**) in good yield, confirming the dimethylethene function as a suitable electron donor.[22]

However, $\mathbf{7}^{\bullet+}$ is of interest also because it offers a less biased test for a seven-membered transition state than the formation of **17** from $\mathbf{6}^{\bullet+}$. Radical ion $\mathbf{7}^{\bullet+}$ lacks the *Z*-arrangement of $\mathbf{6}^{\bullet+}$, which limits the hydroxy function to the same hemisphere as the dimethylethylene target. In contrast, the reactive groups of $\mathbf{7}^{\bullet+}$ have a full complement of conformers accessible and have to meet by conformational diffusion. Again, $\mathbf{7}^{\bullet+}$ has the potential to form, in addition, an eight-membered ring system. The fact that this was not realized has thermodynamic as well as kinetic reasons. Energetic reasons favor the product formed via 7-O–C-cy-**7**, because it has a tertiary free radical site compared to the secondary site of 8-O–Ccy-$\mathbf{7}^{\bullet}$. Conformational/kinetic reasons, such as the precedent of the Dieckmann condensation,[19] further argue against the eight-membered transition state as a viable option.

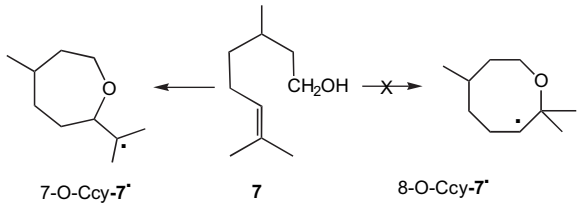

We note, however, that a nucleophilic substitution via an eight-membered transition state has been achieved by Floreancig and co-workers. In this reaction a benzyl group is being replaced by a tethered hydroxy function (vide infra).[32] The intramolecular substitution in the system studied does not have the option of a competing pathway, which may be more favorable for either energetic or kinetic reasons.

4.2. Chrysanthemol and homochrysanthemol radical cations—nucleophilic substitution versus nucleophilic capture

The second group of target molecules is comprised of chrysanthemol and homochrysanthemol, whose radical cations, $\mathbf{8}^{\bullet+}$ and $\mathbf{9}^{\bullet+}$, offer two different cases of competing pathways between nucleophilic substitution and capture. As derivatives of vinylcyclopropane, the distribution of spin and charge in these species is of special interest. The radical cation of the parent system is of a very special structure type: spin and charge are delocalized between the vinyl group and the tertiary cyclopropane carbon (Fig. 6).[33] This radical cation is one of the few cyclopropane species with two lengthened ring bonds.[3a,c,d,17,33]

The additional substituents in $\mathbf{8}^{\bullet+}$ and $\mathbf{9}^{\bullet+}$ distort the symmetry and affect the distribution of spin and charge. The nature of $\mathbf{8}^{\bullet+}$ was probed by chemically induced dynamic nuclear polarization (CIDNP), an NMR technique that allows one to derive patterns of hyperfine coupling constants of free

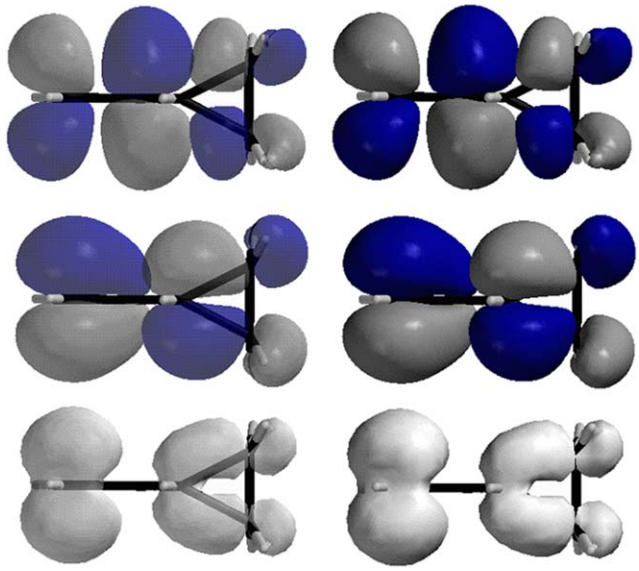

Figure 6. Stereoview of unpaired spin density (bottom), SOMO (center) and LUMO (top) for the radical cation of vinylcyclopropane.[32]

radicals and radical ions from enhanced NMR spectra, observed in emission and/or absorption, during radical (ion) pair reactions.[34] The CIDNP spectrum of the electron transfer reaction from **8** to photo-excited chloranil (Fig. 7) shows that the spin density of $\mathbf{8}^{\bullet+}$ is extended to C-1. This assignment is confirmed by the HOMO and LUMO coefficients of $\mathbf{8}^{\bullet+}$ (Fig. 8).[23]

The SOMO and LUMO coefficients of $\mathbf{8}^{\bullet+}$ and the distribution of spin and charge are such that nucleophilic substitution is possible at two cyclopropane carbons, C-2 and C-3. In addition, nucleophilic capture of the β-carbon in the 2-methylpropenyl side chain is feasible. We evaluate the probability of the potential pathways by considering steric

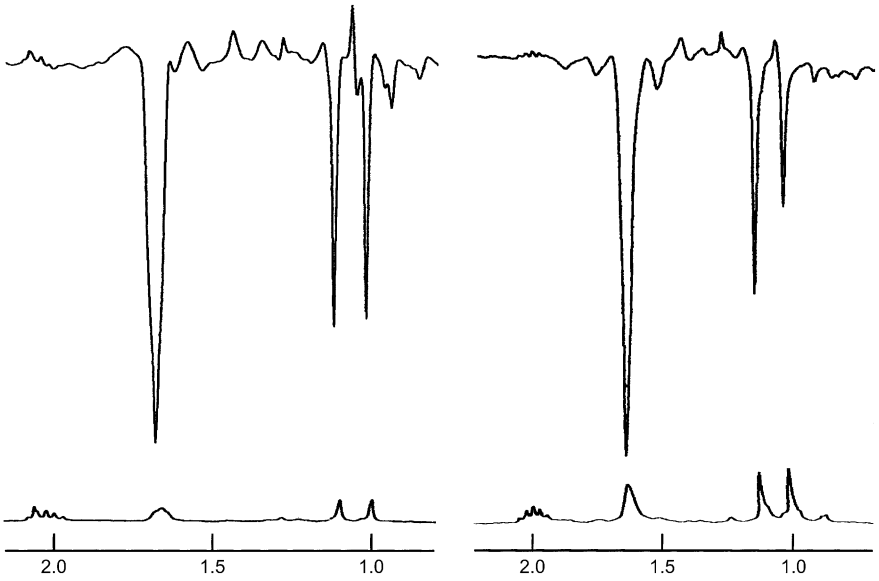

Figure 7. ^{1}H CIDNP spectra observed during irradiation of chloranil solutions in acetonitrile in the presence of *cis*- (left) and *trans*-chrysanthemol, **8** (right).[23] The spectra support radical cations of very similar spin density distributions. The signals representing the two pairs of non-equivalent methyl groups at ~1.6 and at 1.1 and 1.0 ppm, respectively, show strong emission; the single olefinic resonance appears in weak emission (not shown). The allylic cyclopropane proton (1.25 ppm) and the proton adjacent to the hydroxymethyl group show negligible polarization.

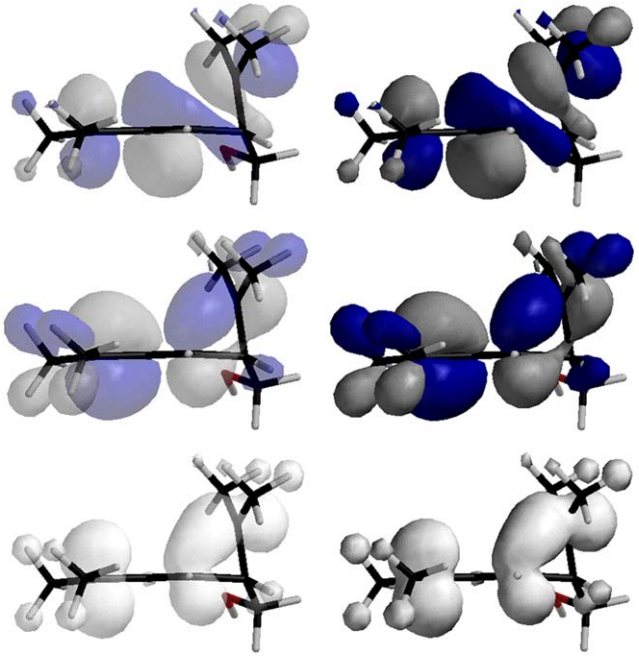

Figure 8. Stereoview of unpaired spin density (bottom), SOMO (center) and LUMO (top) for *cis*-chrysanthemol radical cation, **8**$^{\bullet+}$.[23]

and energetic factors. Substitution at C-2 generates 4-NuS-**8**$^{\bullet}$; substitution at C-3 generates 4′-NuS-**8**$^{\bullet}$ with inversion of configuration at C-3; finally, nucleophilic capture at the β-carbon forms 6-NuC-**8**$^{\bullet}$; the configuration at C-1 is retained in all three reactions.[23]

The two pathways leading to oxetane formation do not appear favorable, because they involve replacing a three-membered ring by a four-membered one with negligible change in strain energy. The pathway leading to 4′-NuS-**8**$^{\bullet}$ is particularly unfavorable, because it generates an isolated radical site, albeit a tertiary one, and a double bond rather than an allylic radical, as in 4-NuS-**8**$^{\bullet}$. For both reactions, the trajectory of approach is far from the ideal 180°. On the other hand, the nucleophilic capture at the β-carbon offers an unencumbered six-membered transition state, which has an additional opportunity of stabilization by subsequent ring opening with formation of a tertiary free radical as an intramolecular leaving group. Formally, the overall mechanism belongs to the elusive S_N2' type. In view of these considerations, it is hardly surprising that **8**$^{\bullet+}$, exclusively forms 6-NC-**8**$^{\bullet}$.[23] The final product, **19**, once again is formed by aromatic substitution (cf., Scheme 2, Eq. 7).

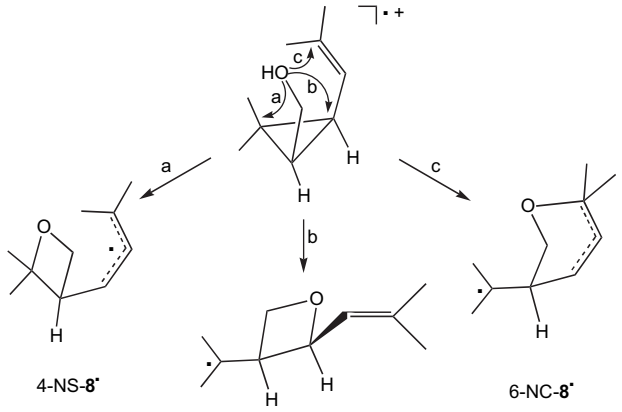

We illustrate the conformational challenges to intramolecular nucleophilic substitution by exploring the conformational hypersurface of **8**$^{\bullet+}$ using density functional theory (DFT) methods. The lowest energy conformer of radical cation **8**$^{\bullet+}$ is one in which the hydroxyl function is deployed far from either electron deficient center, C-2 or Cβ (Fig. 9). Rotation of the 2-methylpropenyl function around the C-3–C-1′ bond results in a complex conformational profile; for comparison, the distance between the oxygen atom and C-2 is shown for selected conformers (Fig. 10).

The case of homochrysanthemol radical cation, **9**$^{\bullet+}$, is different because the two reaction types, substitution and capture, now proceed via five- and seven-membered transition states, respectively. This changes the energetic and conformational features for both. Nucleophilic substitution now becomes favorable because of a five-membered transition state in which an allyl radical is an intramolecular leaving group.[24] On the other hand, capture of the β-carbon, generating 7-NuC-**9**$^{\bullet}$, now is encumbered by the presumably less favorable seven-membered transition state.[24] As a consequence of

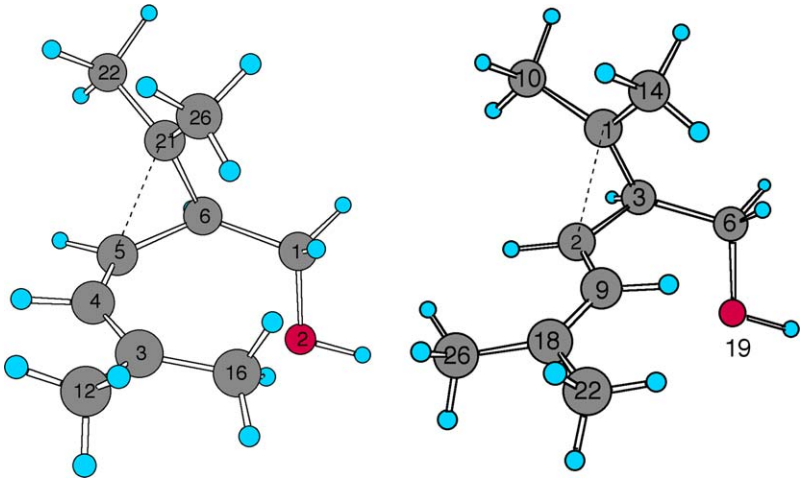

Figure 9. cis,*syn*,*syn*-Conformer (left) and cis,*syn*,*anti*-conformer of *cis*-chrysanthemol radical cation, *cis*-**8**$^{\bullet+}$ (right) calculated by DFT methods (6-31G* basis set).

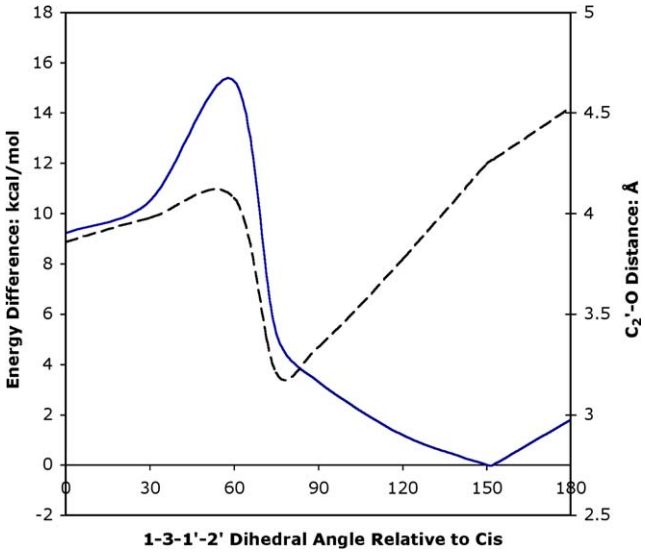

Figure 10. Conformational profile of *cis*,*syn*-chrysanthemol, *cis*,*syn*-**8**$^{\bullet+}$, for rotation around the bond between C-3 and C-1′ (—, solid curve) and C-2′–O distance as a function of dihedral angle (- - -, dashed curve). The geometries of seven individual conformers were calculated by DFT methods (6-31G* basis set).

the changed energetics compared to **8**$^{\bullet+}$, the reaction of **9**$^{\bullet+}$ takes a different course: it proceeds exclusively via the five-membered transition state, producing 5-NuS-**9**$^{\bullet}$. The final product, **20**, once again is formed by aromatic substitution (Scheme 2, Eq. 7).

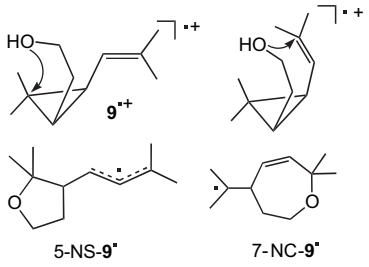

The intramolecular nucleophilic substitution of **9**$^{\bullet+}$ was not without precedent. A bicyclic system, 1-(3-hydroxypropyl)-bicyclo[4.1.0]heptane radical cation, **30**$^{\bullet+}$, was known to form the spiro-fused ether, **31**. This reaction also involves a five-membered transition state, 5-NuS-**30**$^{\bullet+}$; it proceeds by backside attack with inversion of configuration and retention of chirality.[35] In principle, **30**$^{\bullet+}$ could also react via a six-membered transition state, viz. 6-NuS-**30**$^{\bullet+}$, but the approach of the OH function would have to follow a trajectory far from the ideal 180°. Furthermore, this pathway does not benefit from the favorable loss of benzyl radical (Scheme 3).

Results observed in the photo-induced electron transfer reaction of 1-(4-hydroxypentyl)-4-methyl-2,3-diazabicyclo-[2.2.1]hept-2-ene, **32**, provide an interesting complement to those observed for **30**. Radical cation, **32**$^{\bullet+}$, yields a [6.4]spiro-fused six-membered ether, **34**, via the deazetized radical cation **33**$^{\bullet+}$.[36] This product arises by backside attack, via a six-membered transition state, 6-NuS-**33**$^{\bullet+}$, with a trajectory near 180°. The rigid steric requirements for intramolecular nucleophilic substitution (as well as for nucleophilic

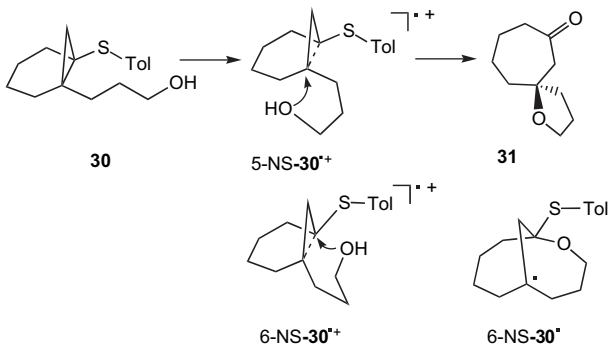

Scheme 3.

substitution in general) are further illustrated by the failure of **33**$^{\bullet+}$ to yield products that could arise via the seven-membered transition state, 7-NuS-**33**$^{\bullet+}$ (Scheme 4).

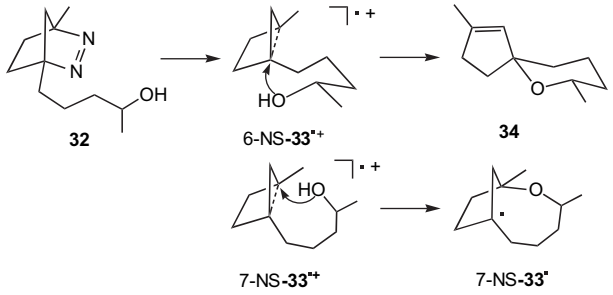

Scheme 4.

A system similar to **32**, but with a side chain extended by one methylene group, might be useful to probe the feasibility of nucleophilic substitution via a seven-membered transition state, although the approach of the OH function generating the bridgehead free radical 7-NuS-**35**$^{\bullet}$ might have a trajectory deviating from the ideal 180°. A reaction of this type was realized by Floreancig (vide infra).

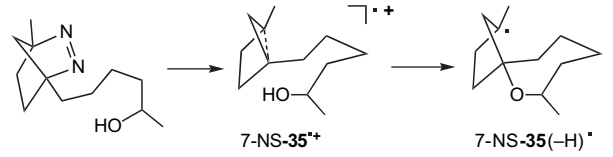

Arnold and co-workers evaluated the intramolecular nucleophilic capture of 6-methyl-5-hepten-2-ol, **36**$^{\bullet+}$, 6-methyl-6-hepten-2-ol, **37**$^{\bullet+}$, and terpineol [4-(1-hydroxy-1-methylethyl)cyclohexene] radical cations, **38**$^{\bullet+}$.[37] Their results were published essentially simultaneously[38] with our work on geraniol[22a] and chrysanthemol.[23] The systems studied can form tetrahydrofuran or pyran rings via five- or six-membered transition states, respectively. The five-membered transition state is favored significantly: the internal alkene, **36**$^{\bullet+}$, exclusively forms the tetrahydrofuran; the terminal alkene, **37**$^{\bullet+}$, preferentially forms the tetrahydrofuran ring, even though this reaction requires formation of a primary radical (!); finally, the terpene, **38**$^{\bullet+}$, prefers the five-membered transition state by a ratio of 10:1.

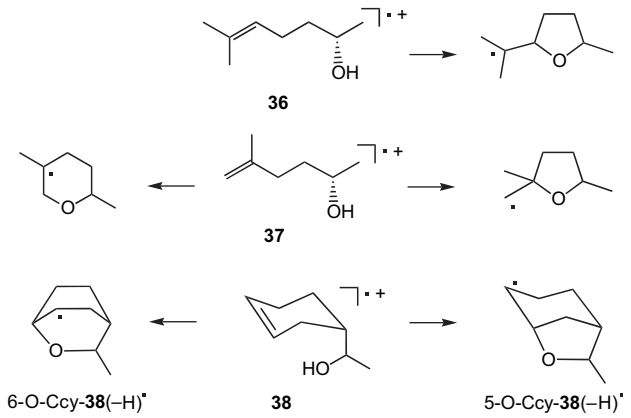

More recently, O–C cyclizations yielding five- through eight-membered rings have been accomplished, in which benzyl groups, the primary seat of spin and charge, act as leaving groups for the tethered hydroxyl function; an alkoxy group at the electrophilic center serves to further weaken the benzylic bond.[32] These studies included one case of an intramolecular competition between five- and six-membered transition states. Substrate **39**, which has hydroxyl functions in both γ- and δ-positions, clearly prefers the formation of the tetrahydrofuran derivative, **40**, compared to the cyclization leading to the pyran derivative. In these reactions the promise of synthetic utility is fulfilled.[32]

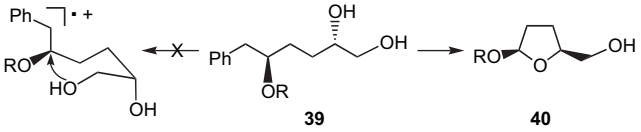

4.3. Electron transfer photosensitized cyclization of *trans*-1-(*o*-hydroxyphenyl)-2-phenylcylopropane

In the light of the preceding discussion, the formation of the dehydrogenated cyclic ether, **21**, upon triphenylpyrylium tetrafluoroborate (**TPT**) sensitized irradiation of *trans*-**10** poses a highly interesting mechanistic problem. The potential intramolecular capture of *trans*-**10**$^{\bullet+}$ is of special interest because it would amount to an unprecedented front-side substitution with retention of configuration. Formally, the required five-membered transition state has precedence (vide supra), but the trajectory is far from the suggested ideal one for nucleophilic substitution.[14]

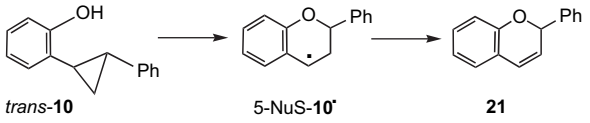

The available evidence supports the intermediacy of the radical cation, *trans*-**10**$^{\bullet+}$. Thus, the oxidation potential of *trans*-**10** is assumed to lie near that of 1,2-diphenylcyclopropane, E_{ox}=1.17 V versus Ag/Ag$^+$;[39] given the reduction potential of **TPT** (E_{red}=−0.29 V vs SCE),[40] electron transfer is energetically feasible to both the excited singlet state, ^{1}**TPT*** ($E_{0,0}$=65 kcal mol^{-1}; $\Delta G\sim$−1.0 eV), and the triplet state, ^{3}**TPT*** (E_T=53 kcal mol^{-1}; $\Delta G\sim$−0.5 eV).[41] In addition, the formal product of intramolecular capture, the benzylic free radical, 5-NuC-**10**$^{\bullet}$, is the likely immediate precursor for **21**.

This leaves the question whether *trans*-**10**$^{\bullet+}$ is the direct precursor for 5-NuC-**10**$^{\bullet}$, or whether the conversion of *trans*-**10**$^{\bullet+}$ into 5-NuC-**10**$^{\bullet}$ proceeds via an additional intermediate and, thus, involves a mechanism other than intramolecular nucleophilic substitution. The electronic structure of *trans*-**10**$^{\bullet+}$ is of major importance in determining its reactivity. Typically, disubstituted cyclopropane radical cations adopt a 'trimethylene' structure in which significant spin and charge reside in one lengthened C–C bond.[2e,3a,d] However, the presence of the *o*-OH function in conjugation with charge and unpaired spin, may change the structure of *trans*-**10**$^{\bullet+}$ to a bifunctional one, e.g., bf-**10**$^{\bullet+}$. The details of this interesting conversion go beyond the scope of this paper. Approaches to gain further insight into the mechanism of this reaction will be reported in a separate paper, including the results of density functional theory (DFT) calculations, laser flash photolysis (LFP), and an evaluation of the reactivity of a related phenoxyl radical, *trans*-**10**$^{\bullet}$ (–H$^{\bullet}$).

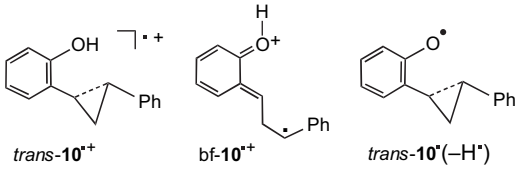

Laser flash photolysis has proved to be an exceedingly valuable tool to probe fast photo-induced conversions. This technique has yielded a wealth of information about free radicals, carbocations, carbenes, or nitrenes.[42] Molecular orbital calculations, either using ab initio or density functional theory (DFT) methods are well suited to elucidate this problem. Structural features such as spin and charge density distribution will delineate the preferred structure type and provide the key to the reactivity of the prevailing species.

4.4. Electron transfer photosensitized cyclization of *endo*-2-hydroxymethylbicyclo[2.2.1]heptene and related compounds

The final intramolecular reaction to be discussed is the intramolecular capture of radical cation, **11**$^{\bullet+}$, derived from *endo*-5-norbornene-2-methanol, which forms the tricyclic ether **22**. Compared to the complex structural and mechanistic problem posed by the reaction of *trans*-**10** this system may appear trivial, but it does command some interest in its own right. We selected this target because of its relationship with norbornadiene and norbornene radical cations, **41**$^{\bullet+}$ and **42**$^{\bullet+}$, respectively, and to the radical cation, **43**$^{\bullet+}$,

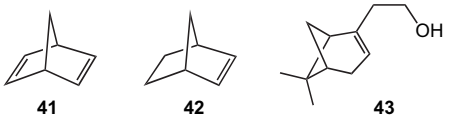

derived from 6,6-dimethylbicyclo[3.1.1]hept-2-ene-2-ethanol (nopol).

Norbornadiene radical cation, **41**$^{\bullet+}$, and its valence isomer, quadricyclane radical cation, undergo a rich variety of reactions with nucleophiles.[43] Interestingly, **41**$^{\bullet+}$ is captured exclusively from the *exo* face,[43a,b] but forms a molecular complex with cyanoaromatic radical anions from the *endo* side.[43c,d] For example, addition of methanol forms a free radical, **41-A**$^{\bullet}$, which is in equilibrium with two isomeric radicals, **41-B**$^{\bullet}$ and **41-C**$^{\bullet}$, by cyclopropylcarbinyl–butenylcarbinyl rearrangements.[43a,b] The free radicals form products by reduction/protonation[43b] (Eq. 5, Scheme 2), hydrogen abstraction[43b] (Eq. 7, Scheme 2), or aromatic substitution (Eq. 6, Scheme 2).[43b]

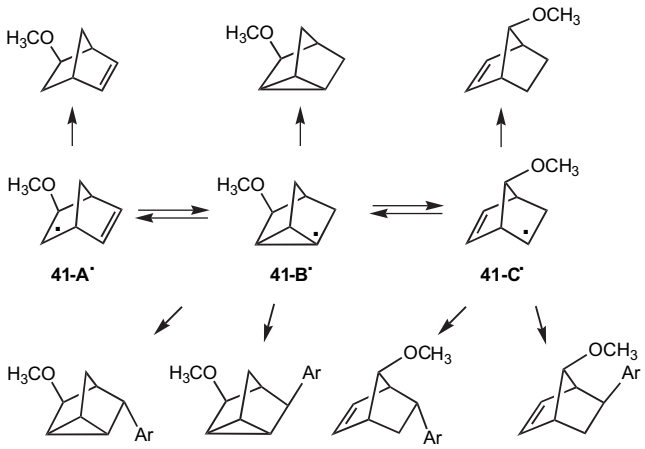

Since norbornene, **42**, on the other hand, is attacked from *endo* and *exo* face,[8c] **11**$^{\bullet+}$ was expected to readily undergo nucleophilic capture. An interesting question concerned the regiochemistry of capture, whether a six-membered transition state might give rise to a tricyclic pyran derivative. The only product isolated from this reaction, **22**, shows that nucleophilic capture via a five-membered transition state prevails; product **22** arises from the tricyclic radical intermediate 5-O–Ccy-**11**(–H)$^{\bullet}$ either by hydrogen abstraction (Eq. 7, Scheme 2) or reduction/protonation (Eq. 5, Scheme 2).[22b]

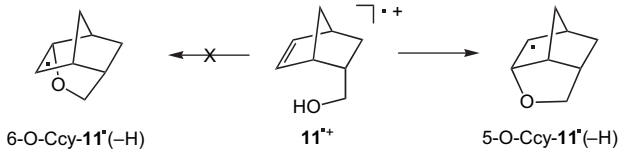

Nopol is one of several vinylcyclobutane systems whose radical cations have attracted attention.[18,44] As was demonstrated particularly clearly for α-pinene radical cation, **44**$^{\bullet+}$, these intermediates delocalize spin and charge between the vinyl group and the cyclobutane ring while retaining their chirality.[45] They are captured by nucleophilic attack on C-6 (→**45**$^{\bullet}$) or give rise to unusual 'substitution' products, e.g., **46**, which are initiated by deprotonation.[44,45] The dehydrogenation product, verbenene, **47**, also can be rationalized via deprotonation (Scheme 5).[44,45]

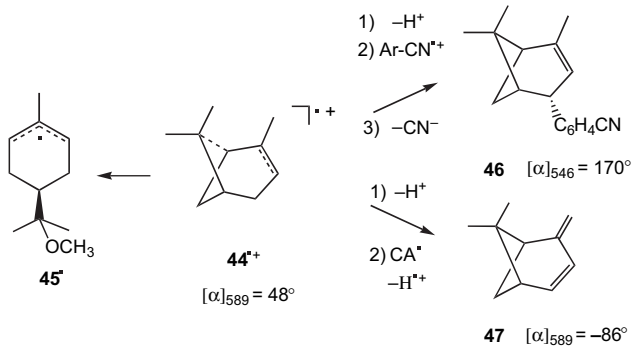

Scheme 5.

Nopol radical cation, **43**$^{\bullet+}$, has two potential pathways for intramolecular nucleophilic reaction, capture at C-3 (→**49**$^{\bullet}$) and substitution at C-1 (→**48**$^{\bullet}$). Given the fact that significant charge density is removed from the alkene function, it may not be too surprising that **43**$^{\bullet+}$ fails to undergo capture. In addition, this reaction will reintroduce any ring strain partially relieved by delocalizing spin and charge into the C-1–C-6 bond. The failure to undergo intramolecular substitution may have steric reasons; the required transition state is different from 5-NuS-**30**$^{\bullet+}$ (vide supra), because three atoms are fixed leaving only rotations around two bonds to align the nucleophile for the required trajectory. Given the relatively high energy calculated for intermediate 5-NuS-**10**$^{\bullet+}$ in the analogous reaction of **10**, it is understandable that **43**$^{\bullet+}$ only reacts with intermolecular nucleophiles (→**52**$^{\bullet}$; Scheme 6).[18]

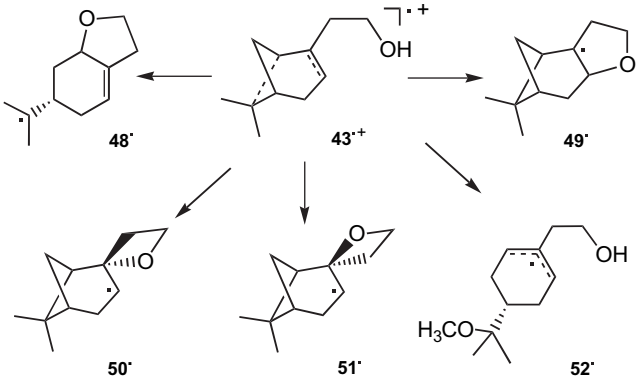

Scheme 6.

Concerning the relationship of **11**$^{\bullet+}$ to **43**$^{\bullet+}$, the analogy is but a formal one, a hydroxyl function attached in a fashion that would allow a five-membered transition state for nucleophilic capture or substitution. The difference in reactivity can be ascribed to the steric and electronic features that set the reactions of **43**$^{\bullet+}$ apart from those of **11**$^{\bullet+}$. One significant difference that might contribute to the eventual outcome of the reactions, lies in the fact that **11**$^{\bullet+}$ reacts by a Baldwin-5-*exo-trig* process, whereas the conversion of **43**$^{\bullet+}$ to **49**$^{\bullet}$ proceeds via a 5-*endo-trig* process. We ignore the 4-*exo-trig* closure, which would generate a spiro-fused system. There is only one analog for this reaction, the formation of 6,4-tan-**6**$^{\bullet}$ from 6-C–C-cy-**6**$^{\bullet+}$ (vide supra), where the OH function is captured by an empty p orbital. However, the analogy is remote, as it does not involve a nucleophilic substitution.

5. Conclusion

The seven systems, **5**–**11**, investigated in our laboratory and additional systems, **30**, **32**, **36**–**39**, and **43**, reported in the literature, provide a consistent framework for the understanding of intramolecular nucleophilic substitution and capture of alkene and strained ring systems and offer guidelines for further studies. The target molecules form mono-, di-, and tricyclic ethers via four to seven-membered transition states. Not surprisingly, the majority of cyclizations proceed via five- and six-membered transition states for both substitution and capture. A four-membered transition state is realized only in one system: the bicyclic oxetane, **16**, is formed following the C–C cyclization of nerol radical cation, **6**$^{\bullet+}$, which places a hydroxy group in close proximity to a carbocationic site with no alternative cyclization accessible.

Two of the systems studied react via seven-membered transition states; in both cases competing reactions via eight-membered transition states are avoided. The outcome of the competition does not reflect kinetic factors alone; the formation of the eight-membered ethers is also unfavorable thermodynamically. Nerol radical cation, **6**$^{\bullet+}$, forms a seven-membered ether in competition with C–C cyclizations forming five- and six-membered rings. For homochrysanthemol radical cation, **8**$^{\bullet+}$, nucleophilic substitution via a five-membered transition state is preferred over nucleophilic capture via a seven-membered transition state. Finally the formation of dihydropyran, **21**, from *trans*-1-(*o*-hydroxyphenyl)-2-phenylcyclopropane, *trans*-**10**, poses an intriguing mechanistic puzzle.

6. Experimental

6.1. Materials

Three hydroxy-substituted substrates, **5**–**7**, are available commercially (Aldrich). Chrysanthemol, **8**, was prepared by LiAlH reduction of the methyl chrysanthemate prepared from a commercially available mixture of *cis*- and *trans*-chrysanthemic acid (Aldrich). Homochrysanthemol, **9**, was prepared by LiAlH reduction of the methyl ester of homochrysanthemic acid, which was prepared by Arndt–Eistert homologation of chrysanthemic acid, **Ex-1**.[46] The crude diazoketone, **Ex-2**, obtained by treatment of **Ex-3** with thionyl chloride, followed by reaction with diazomethane[47] was heated in methanol solution in the presence of silver benzoate.[48]

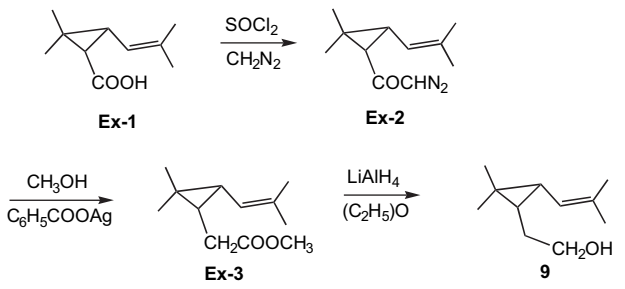

Diarylcyclopropane *trans*-**10** was prepared by a sequence of reactions, initiated by Claisen–Schmidt condensation of benzaldehyde with *o*-hydroxy-acetophenone; condensation of the resulting chalcone with hydrazine hydrate generated a pyrazoline,[49,50] which was deazetized under basic conditions.[51] A mixture of *endo*- and *exo*-5-norbornene-2-methanol (Aldrich) was used without separation because the presence of the *exo*-isomer was not expected to interfere with the chemistry of *endo*-**11**$^{\bullet+}$.

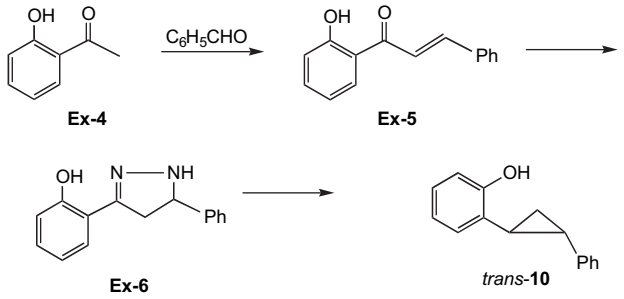

The electron acceptor/sensitizers, 1,4-dicyanobenzene (Aldrich; 98%) and phenanthrene (Aldrich; 98%) were purified by recrystallization. 9,10-Dicyanoanthracene (Eastman Kodak) was purified by recrystallization from acetonitrile. Acetonitrile (Fischer), methanol (Fischer), and methylene chloride (Fischer; Spectranalyzed®) were distilled from calcium hydride and stored over 4A molecular sieves in brown bottles under argon atmosphere.

6.2. Electron transfer photosensitized reactions—irradiation procedures

Solutions containing 0.1 M of donors **1**–**5** or **7** and either 0.1 M of 1,4-dicyanobenzene/0.02 M phenanthrene or 0.1 M of 9,10-dicyanoanthracene/0.02 M biphenyl as sensitizer/co-sensitizer in acetonitrile or methylene chloride were deoxygenated by purging with argon for 15 min and irradiated in a Rayonet RPR-100 photoreactor equipped with 16 RPR-3500 lamps. The progress of the reaction was monitored by gas chromatography on a GC/MS system (HP 5890 series II GC interfaced with an HP 5971 mass selective detector), using a 12 m×0.2 mm×0.33 μm HP-1 capillary column (cross-linked methyl silicone on fused silica). Exploratory runs were carried out in 4-mm ID NMR tubes capped with latex stoppers, preparative runs in 30-mm ID tubes with central cooling fingers (water-cooling).

For donor **6** exploratory experiments were carried out by irradiating solutions of 0.02 g substrate in 20 mL methylene chloride with triphenylpyrilium tetrafluoroborate in 10% molar ratio under argon for 1 h in Pyrex tubes surrounding a central quartz cooling jacket with a 125-W medium-pressure mercury lamp. For preparative runs solutions of 1.0 g of the substrate in 400 mL freshly distilled methylene chloride were irradiated at ambient temperature with a 125-W medium-pressure mercury lamp inside a quartz immersion well.

6.3. Isolation of reaction products

Reaction products obtained in yields>5% were isolated by chromatography on columns, 1 cm<ID<5 cm, packed with ~15-cm of TLC standard grade silica gel (Aldrich; without

binder), and eluted with solvent gradients, usually from light petroleum ether (bp<65 °C) to mixtures with either methylene chloride or ethyl acetate. Several passes were required to isolate the products.

The product resulting from *trans*-**10** was isolated and purified by conventional column chromatography on silica gel Merck 60 (0.063–0.200 mm), by preparative layer chromatography on silica gel Merck 60 PF_{254}, using dichloromethane as eluent, or by means of isocratic HPLC equipment fitted with a semi-preparative Microporasil column, using hexane/ethyl acetate as eluent.

6.4. Characterization/identification of products

Structure assignments of isolated products rest on MS and NMR data, including DEPT, two-dimensional COSY, and HETCOR experiments, where appropriate. NOE difference spectra were recorded to elucidate the substituent stereochemistry and the spatial relationship between the various functional groups. ^{1}H NMR spectra ($CDCl_3$; δ, ppm downfield of TMS) were recorded on a Varian XL-400, a 300 MHz Varian Gemini instrument, or a Varian VXR-200 spectrometer. ^{13}C and HETCOR spectra were recorded on the Varian VXR-200 spectrometer operating at 50.3 MHz. IR spectra were recorded on a GC–FTIR Hewlett-Packard 5965; the major bands are characterized by their ν_{max} (cm^{-1}). Mass spectra were obtained using a Hewlett-Packard 5988 A spectrometer.

6.5. Computational details

Density functional theory (DFT) and/or ab initio calculations[52] were carried out with the GAUSSIAN 03 series of electronic structure programs,[53] in some cases with earlier versions, using extended basis sets, including p-type polarization functions on carbon (6-31G*). The geometries of the neutral parent molecules and radical cations were optimized at the unrestricted Hartree-Fock (UHF/6-31G*//UHF/6-31G*) and UB3LYP/6-31G* levels, respectively. Previous experience suggests that this level of theory will reproduce the major geometric features of the systems under study. Some radical cations were also calculated to include higher degrees of electron correlation at the MP2 level of theory (MP2/6-31G*//MP2/6-31G*). Wavefunction analyses for charge and spin density distributions used the conventional Mulliken partitioning scheme.[52]

Møller–Plesset perturbation theory (MP2) reproduces *positive* ^{1}H hyperfine coupling constants satisfactorily, but overestimates spin densities on carbon and negative hfcs significantly, often by factors>2.[54–57] On the other hand, density functional theory methods[59] give satisfactory agreement with experimental results.[58–60] Indeed, positive and negative hfcs of norbornadiene, quadricyclane, and bicyclobutane radical cations are reproduced accurately with either the (B3LYP/6-31G*//MP2/6-31G*) or the (B3LYP/6-31G*//B3LYP/6-31G*) method.[58–60] In selected cases, including the radical cations of 1,2-dimethylcyclopropane, norcaradiene, vinylcyclopropane, and chrysanthemol, pictorial representations of spin density, SOMO and LUMO were derived with the program SPARTAN.[61] The previously optimized MP2/6-31G* geometries were imported into SPARTAN, an HF/6-31G* single point calculation was carried out followed by a surface analysis for spin density, SOMO and LUMO.

Acknowledgements

H. D. Roth thanks NSF (Grant NSF-97-14850) and gratefully acknowledges an IBERDROLA Award. R. R. Sauers thanks the National Center for Supercomputer Applications for an allocation of time on the IBM P Series 690 (Grant CHE030060).

References and notes

1. (a) *Radical Ions*; Kaiser, E. T., Kevan, L., Eds.; Interscience: New York, NY, 1968; (b) Forrester, R. A.; Ishizu, K.; Kothe, G.; Nelsen, S. F.; Ohya-Nishiguchi, H.; Watanabe, K.; Wilker, W. Organic Cation Radicals and Polyradicals. In *Landolt-Börnstein, Numerical Data and Functional Relationships in Science and Technology*; Springer: Heidelberg, 1980; Vol. IX, Part d2; (c) Yoshida, K. *Electrooxidation in Organic Chemistry: The Role of Cation Radicals as Synthetic Intermediates*; Wiley: New York, NY, 1984; (d) Shida, T. *Electronic Absorption Spectra of Radical Ions*; Elsevier: Amsterdam, 1988; (e) *Radical Ionic Systems*; Lund, A., Shiotani, M., Eds.; Kluwer Academics: Dordrecht, The Netherlands, 1991; In addition, SciFinder Scholar retrieves 2352 papers on the chemistry, spectroscopy, and physics of *radical cations* in the first four years of the current millennium alone.
2. (a) Ledwith, A. *Acc. Chem. Res.* **1972**, *5*, 133–139; (b) Shida, T.; Haselbach, E.; Bally, T. *Acc. Chem. Res.* **1984**, *17*, 180–186; (c) Nelsen, S. F. *Acc. Chem. Res.* **1987**, *20*, 269–276; (d) Bauld, N.; Bellville, D. J.; Harirchian, B.; Lorenz, K. T.; Pabon, R. A., Jr.; Reynolds, D. W.; Wirth, D. D.; Chiou, H.-S.; Marsh, B. K. *Acc. Chem. Res.* **1987**, *20*, 180–186; (e) Roth, H. D. *Acc. Chem. Res.* **1987**, *20*, 343–370; (f) Mangione, D.; Arnold, D. R. *Acc. Chem. Res.* **2002**, *35*, 297–304.
3. (a) Makosza, M. *Pure Appl. Chem.* **1997**, *69*, 559; (b) Makosza, M.; Wojciechowski, K. *Liebigs Ann.-Rcl.* **1997**, *9*, 1805; (c) Makosza, M.; Wojciechowski, K. *Heterocycles* **2001**, *54*, 445; (d) Makosza, M.; Wojciechowski, K. *Chem. Rev.* **2004**, *104*, 2631.
4. (a) Takahashi, Y.; Mukai, T.; Miyashi, T. *J. Am. Chem. Soc.* **1983**, *105*, 6511–6513; (b) Miyashi, T.; Takahashi, Y.; Mukai, T.; Roth, H. D.; Schilling, M. L. M. *J. Am. Chem. Soc.* **1985**, *107*, 1079–1080; (c) Gassman, P. G.; Hay, B. A. *J. Am. Chem. Soc.* **1985**, *107*, 4075–4076; (d) Gassman, P. G.; Hay, B. A. *J. Am. Chem. Soc.* **1986**, *108*, 4227–4228; (e) Arnold, A.; Burger, U.; Gerson, F.; Kloster-Jensen, E.; Schmidlin, S. P. *J. Am. Chem. Soc.* **1993**, *115*, 4271–4281.
5. (a) Gassman, P. G.; Hay, B. A. *J. Am. Chem. Soc.* **1985**, *107*, 4075; (b) Gassman, P. G.; Hay, B. A. *J. Am. Chem. Soc.* **1986**, *108*, 4227.
6. Arnold, A.; Burger, U.; Gerson, F.; Kloster-Jensen, E.; Schmidlin, S. P. *J. Am. Chem. Soc.* **1993**, *115*, 4271–4281.
7. (a) Adam, W.; Walter, H.; Chen, G.-F.; Williams, F. *J. Am. Chem. Soc.* **1992**, *114*, 3007–3014; (b) Weng, H.; Sethuraman, V.; Roth, H. D. *J. Am. Chem. Soc.* **1994**, *116*, 7021–7025; (c) Weng, H.; Sheik, Q.; Roth, H. D. *J. Am. Chem. Soc.* **1995**, *117*, 10655–10661.

8. (a) Neunteufel, R. A.; Arnold, D. R. *J. Am. Chem. Soc.* **1973**, *95*, 4080–4081; (b) Maroulis, A. J.; Shigemitsu, Y.; Arnold, D. R. *J. Am. Chem. Soc.* **1978**, *100*, 535–541; (c) Arnold, D. R.; Snow, M. S. *Can. J. Chem.* **1988**, *66*, 3012–3026; (d) Arnold, D. R.; Du, X. *J. Am. Chem. Soc.* **1989**, *111*, 7666–7667.
9. (a) Klett, M.; Johnson, R. P. *J. Am. Chem. Soc.* **1985**, *107*, 6615–6620; (b) Rao, V. R.; Hixson, S. S. *J. Am. Chem. Soc.* **1979**, *101*, 6458–6459; (c) Mizuno, K.; Ogawa, J.; Otsuji, Y. *Chem. Lett.* **1981**, 742–744; (d) Hixson, S. S.; Xing, Y. *Tetrahedron Lett.* **1991**, *32*, 173–174.
10. (a) Mattes, S. L.; Farid, S. *Org. Photochem.* **1983**, *6*, 233–326; (b) Lewis, F. D. *Photoinduced Electron Transfer*; Fox, M. A., Chanon, M., Eds.; Elsevier: Amsterdam, 1988; Part C, Chapter 4.1; (c) Bauld, N. L. *Adv. Electron Transfer Chem.* **1992**, *2*, 1.
11. (a) Maslak, P.; Asel, S. A. *J. Am. Chem. Soc.* **1988**, *110*, 8260–8261; (b) Maslak, P.; Asel, S. A. *Angew. Chem., Int. Ed. Engl.* **1990**, *29*, 8260–8261.
12. (a) Lorenz, K.; Bauld, N. L. *J. Catal.* **1985**, *95*, 613–616; (b) Roth, H. D.; Schilling, M. L. M. *J. Am. Chem. Soc.* **1985**, *107*, 716–718; (c) Roth, H. D.; Schilling, M. L. M.; Abelt, C. J. *Tetrahedron* **1986**, *42*, 6157–6166; (d) Roth, H. D.; Schilling, M. L. M.; Abelt, C. J. *J. Am. Chem. Soc.* **1986**, *108*, 6098–6099; (e) Miyashi, T.; Konno, A.; Takahashi, Y. *J. Am. Chem. Soc.* **1988**, *110*, 3676–3677.
13. (a) Dinnocenzo, J. P.; Schmittel, M. *J. Am. Chem. Soc.* **1987**, *109*, 1561–1562; (b) Dinnocenzo, J. P.; Conlon, D. A. *J. Am. Chem. Soc.* **1988**, *110*, 2324–2326; (c) Dinnocenzo, J. P.; Todd, W. P.; Simpson, T. R.; Gould, I. R. *J. Am. Chem. Soc.* **1987**, *109*, 1561–1562; (d) Dinnocenzo, J. P.; Todd, W. P.; Simpson, T. R.; Gould, I. R. *J. Am. Chem. Soc.* **1990**, *112*, 2462–2464.
14. (a) Shaik, S. S.; Dinnocenzo, J. P. *J. Org. Chem.* **1990**, *55*, 3434–3436; (b) Shaik, S. S.; Reddy, A. C.; Ioffe, A.; Dinnocenzo, J. P.; Danovich, D.; Cho, J. K. *J. Am. Chem. Soc.* **1995**, *117*, 3205–3222.
15. Wlostowski, M.; Roth, H. D. Unpublished results, cited in Roth, H.D., Ref. 3d.
16. Herbertz, T.; Roth, H. D. Unpublished results, cited in Roth, H.D., Ref. 3d.
17. Herbertz, T.; Blume, F.; Roth, H. D. *J. Am. Chem. Soc.* **1998**, *120*, 4591–4599.
18. Arnold, D. R.; Du, X. *Can. J. Chem.* **1994**, *72*, 403–414.
19. Schaefer, J. P.; Bloomfield, J. J. *Org. React.* **1967**, *15*, 1–203.
20. Makosza, M.; Owczarczyk, Z. *J. Org. Chem.* **1989**, *54*, 5094.
21. (a) Makosza, M.; Goliński, J.; Baran, J. *J. Org. Chem.* **1984**, *49*, 1488; (b) RajanBabu, T. V.; Reddy, G. S.; Fukunaga, T. *J. Am. Chem. Soc.* **1985**, *107*, 5473; (c) Makosza, M.; Białecki, M. *J. Org. Chem.* **1998**, *63*, 4878.
22. (a) Weng, H.; Scarlata, C.; Roth, H. D. *J. Am. Chem. Soc.* **1996**, *118*, 10947–10953; (b) Weng, H. Ph.D. Thesis, Rutgers University, 1996.
23. Herbertz, T.; Roth, H. D. *J. Am. Chem. Soc.* **1996**, *118*, 10954–10962.
24. Herbertz, T.; Roth, H. D. *J. Org. Chem.* **1999**, *64*, 3708–3713.
25. Delgado, J.; Espinós, A.; Jiménez, M. C.; Miranda, M. A.; Roth, H. D.; Tormos, R., unpublished results.
26. (a) Goldschmidt, C. R.; Potashnik, R.; Ottolenghi, M. *J. Phys. Chem.* **1971**, *75*, 1025–1031; (b) Ottolenghi, M. *Acc. Chem. Res.* **1973**, *6*, 153–160; (c) Schomburg, H.; Staerk, H.; Weller, A. *Chem. Phys. Lett.* **1973**, *21*, 433; (d) Taylor, G. N. Unpublished results, cited in Roth H.D. *Mol. Photochem.* 1973, 5, 91–126. (e) Schulten, K.; Staerk, H.; Weller, A.; Werner, H. J.; Nickel, H. *Z. Phys. Chem. NF* **1976**, *101*, 371–390; (f) Roth, H. D.; Schilling, M. L. M. *J. Am. Chem. Soc.* **1980**, *102*, 6805–6811; (g) Karki, S. B.; Dinnocenzo, J. P.; Farid, S.; Goodman, J. C.; Gould, I.; Zona, T. A. *J. Am. Chem. Soc.* **1997**, *119*, 431–432.
27. (a) Roth, H. D. *J. Photochem. Photobiol., C: Photochem. Rev.* **2001**, *2*, 93–116; (b) Roth, H. D. *Pure Appl. Chem.* **2005**, *77*, 1075–1085.
28. The aromatic substitution products, *E*,*E*-, *E*,*Z*-, *Z*,*E*-, and *Z*,*Z*-**12** (R=C_6H_4–CN), are the first of several examples for this product type in this paper. For simple systems, the overall reaction sequence generating them has been dubbed NOCAS, for Nucleophile-Olefin-Combination-Aromatic-Substitution. In French NOCAS is converted to its mirror image, SACON, for Substitution Aromatique avec Combinaison d'une Oléfin et d'une Nucléophile. In the spirit of this acronym, the above reaction is a Tandem-Cyclization-Intramolecular-Nucleophilic-Capture-Aromatic-Substitution or TCINCAS (a creative mind has no limits designing awkward acronyms).
29. Hoffmann, U.; Gao, Y.; Pandey, B.; Klinge, S.; Warzecha, K. D.; Krueger, C.; Roth, H. D.; Demuth, M. *J. Am. Chem. Soc.* **1993**, *115*, 10358–10359.
30. (a) Guo, Q.-X.; Qin, X.-Z.; Wang, J. T.; Williams, F. *J. Am. Chem. Soc.* **1988**, *110*, 1974–1976; (b) Ikeda, H.; Minegishi, T.; Miyashi, T.; Lakkaraju, P. S.; Sauers, R. R.; Roth, H. D. *J. Phys. Chem. B* **2005**, *109*, 2504–2511.
31. Williams, F.; Guo, Q.-X.; Kolb, T. M.; Nelsen, S. F. *J. Chem. Soc., Chem. Commun.* **1989**, 1835–1836.
32. (a) Kumar, V. S.; Floreancig, P. E. *J. Am. Chem. Soc.* **2001**, *123*, 3842–3843; (b) Wang, L.; Seiders, J. R., II; Floreancig, P. E. *J. Am. Chem. Soc.* **2004**, *126*, 12596–12603.
33. Herbertz, T.; Roth, H. D. *J. Am. Chem. Soc.* **1998**, *120*, 11904–11911.
34. (a) Closs, G. L. *Adv. Magn. Reson.* **1974**, *7*, 157–229; (b) Kaptein, R. *Adv. Free Radical Chem.* **1975**, *5*, 319–380; (c) Roth, H. D. *Encyclopedia of Nuclear Magnetic Resonance, Vol. 2*; Grant, D. M., Harris, R. K., Eds.; 1996, pp 1337–1350.
35. Takemoto, Y.; Ohra, T.; Koike, H.; Furuse, S.-i.; Iwata, Ch.; Ohishi, H. *J. Org. Chem.* **1994**, *59*, 4727–4729.
36. Adam, W.; Sendelbach, J. *J. Org. Chem.* **1993**, *58*, 5316–5322.
37. (a) McManus, K. A.; Arnold, D. R. *Can. J. Chem.* **1995**, *73*, 2158–2169; (b) Arnold, D. R.; Connor, D. A.; McManus, K. A.; Bakshi, P. K.; Cameron, T. S. *Can. J. Chem.* **1996**, *74*, 602–612.
38. The independent pursuit of these topics is borne out by the dates of submission of the respective publications, June 20 (Ref. 37a) and November 29, 1995 (Ref. 37b), and July 31 (Ref. 22) and October 26, 1995 (Ref. 23). Of course, all four papers were submitted long after Ref. 29 (May 24, 1993).
39. Wong, P. C.; Arnold, D. R. *Tetrahedron Lett.* **1979**, 2101–2104.
40. Saeva, F. D.; Olin, G. R. *J. Am. Chem. Soc.* **1980**, *102*, 299–303.
41. García, H.; Miranda, M. A. *Chem. Rev.* **1994**, *94*, 1063–1089.
42. (a) Johnston, L. J.; Scaiano, J. C.; Sheppard, J. W.; Bays, J. P. *Chem. Phys. Lett.* **1986**, *124*, 493–498; (b) Das, P. K. *Chem. Rev.* **1993**, *93*, 119–144; (c) Hadel, L. M.; Maloney, V. M.; Platz, M. S.; McGimpsey, W. G.; Scaiano, J. C. *J. Phys. Chem.* **1986**, *90*, 2488–2491; (d) Ford, F.; Yazawa, T.; Platz, M. S.; Ratzinger, S.; Fülscher, M. *J. Am. Chem. Soc.* **1998**, *120*, 4430–4438; (e) Pandurangi, R. S.; Lustak, P.; Kuntz, R. R.; Volkert, W. A.; Rogowski, J.; Platz, M. S. *J. Org. Chem.* **1998**, *63*, 9019–9030.
43. (a) Gassman, P. G.; Olsen, K. D. *Tetrahedron Lett.* **1983**, *1*, 19–22; (b) Weng, H.; Roth, H. D. *J. Org. Chem.* **1995**, *60*, 4136–4145; (c) Weng, H.; Roth, H. D. *Tetrahedron Lett.* **1996**, *37*,

4895–4898; (d) Weng, H.; Roth, H. D. *J. Phys. Org. Chem.* **1998**, *11*, 101–108.
44. Zhou, D.; Sheik, M.; Roth, H. D. *Tetrahedron Lett.* **1996**, *37*, 2385–2388.
45. (a) Roth, H. D.; Weng, H.; Zhou, D.; Lakkaraju, P. S. *Acta Chem. Scand.* **1997**, *51*, 626–635; (b) Zhou, D.; Chou, J.; Roth, H. D. *J. Phys. Org. Chem.* **1999**, *12*, 867–874.
46. Crombie, L.; Crossley, J.; Mitchard, D. A. *J. Chem. Soc.* **1963**, 4957–4969.
47. Black, T. H. *Aldrichim. Acta* **1983**, *16*, 3–10.
48. Wiberg, K. B.; Hutton, T. W. *J. Am. Chem. Soc.* **1956**, *78*, 1640–1645.
49. Chattree, N. S.; Sharma, T. C. *Asian J. Chem.* **1994**, *6*, 405–407.
50. Iksanova, S. V. *Geterosikl. Soedin.* **1991**, 1131–1136; Chem. Abstr. **1992**, *116*, 194239s.
51. Gao, C.; Hay, A. S. *Polymer* **1995**, *36*, 5051.
52. Hehre, W. J.; Radom, L.; Schleyer, P. v. R.; Pople, J. A. *Ab Initio Molecular Orbital Theory*; Wiley Interscience: New York, NY, 1986; presents a detailed description of the theoretical methods used in this work.
53. Frisch, M. J.; Trucks, G. W.; Schlegel, H. B.; Scuseria, G. E.; Robb, M. A.; Cheeseman, J. R.; Montgomery, J. A., Jr.; Vreven, T.; Kudin, K. N.; Burant, J. C.; Millam, J. M.; Iyengar, S. S.; Tomasi, J.; Barone, V.; Mennucci, B.; Cossi, M.; Scalmani, G.; Rega, N.; Petersson, G. A.; Nakatsuji, H.; Hada, M.; Ehara, M.; Toyota, K.; Fukuda, R.; Hasegawa, J.; Ishida, M.; Nakajima, T.; Honda, Y.; Kitao, O.; Nakai, H.; Klene, M.; Li, X.; Knox, J. E.; Hratchian, H. P.; Cross, J. B.; Adamo, C.; Jaramillo, J.; Gomperts, R.; Stratmann, R. E.; Yazyev, O.; Austin, A. J.; Cammi, R.; Pomelli, C.; Ochterski, J. W.; Ayala, P. Y.; Morokuma, K.; Voth, G. A.; Salvador, P.; Dannenberg, J. J.; Zakrzewski, V. G.; Dapprich, S.; Daniels, A. D.; Strain, M. C.; Farkas, O.; Malick, D. K.; Rabuck, A. D.; Raghavachari, K.; Foresman, J. B.; Ortiz, J. V.; Cui, Q.; Baboul, A. G.; Clifford, S.; Cioslowski, J.; Stefanov, B. B.; Liu, G.; Liashenko, A.; Piskorz, P.; Komaromi, I.; Martin, R. L.; Fox, D. J.; Keith, T.; Al-Laham, M. A.; Peng, C. Y.; Nanayakkara, A.; Challacombe, M.; Gill, P. M. W.; Johnson, B.; Chen, W.; Wong, M. W.; Gonzalez, C.; Pople, J. A. *Gaussian 03, Revision B.02*; Gaussian: Pittsburgh, PA, 2003.
54. Raghavachari, K.; Haddon, R. C.; Roth, H. D. *J. Am. Chem. Soc.* **1983**, *105*, 3110–3114.
55. Raghavachari, K.; Roth, H. D. *J. Am. Chem. Soc.* **1989**, *111*, 7132–7136.
56. Roth, H. D.; Schilling, M. L. M.; Raghavachari, K. *J. Am. Chem. Soc.* **1984**, *106*, 253–255.
57. Krogh-Jespersen, K.; Roth, H. D. *J. Am. Chem. Soc.* **1992**, *114*, 8388–8394.
58. (a) Eriksson, L. A.; Malkin, V. G.; Malkina, O. L.; Salahub, D. R. *J. Chem. Phys.* **1993**, *99*, 9756–9763; (b) Eriksson, L. A.; Malkin, V. G.; Malkina, O. L.; Salahub, D. R. *Int. J. Quant. Chem.* **1994**, *52*, 879–901.
59. Batra, R.; Giese, B.; Spichty, M.; Gescheidt, G.; Houk, K. N. *J. Phys. Chem.* **1996**, *100*, 18371–18379.
60. Roth, H. D.; Herbertz, T. 1996, unpublished results.
61. *SPARTAN, SGI Version 4.0.4 GL*; Wavefunction: Irvine, CA, 1991–1995; Deppmeier, B. J.; Driessen, A. J.; Hehre, W. J.; Johnson, H. C.; Leonard, J. M.; Yu, J.; Lou, L., Development Staff; Baker, J.; Carpenter, J. E.; Dixon, R. W.; Fielder, S. S.; Kahn, S. D.; Pietro, W. J., Contributors.